Major transitions in early coral development: novel insights enabled by visualisation of a comprehensive transcriptomic dataset for *Acropora millepora*

Ramona Brunner[1,2*], Mila Grinblat[1,2*], Aurelie Moya[1,2*], Sylvain Foret[3‡], David C Hayward[3], Bruno Lapeyre[1,4], **Eldon E Ball**[3], Ira Cooke[2,5], **David J Miller**[1,2]

[1]ARC Centre of Excellence for Coral Reef Studies, James Cook University, Townsville, QLD 4811 Australia
[2]Molecular Genetics Unit, James Cook University, Townsville, QLD 4811 Australia
[3]Research School of Biology, Australian National University, Acton, ACT 2601 Australia
[4]Laboratoire d'excellence CORAIL, Centre de Recherches Insulaires et Observatoire de l'Environnement (CRIOBE), Moorea, B.P. 1013, Papeete, French Polynesia
[5]Department of Marine Biology and Aquaculture, James Cook University, Townsville, QLD 4811 Australia

[‡]Deceased
Email addresses: RB (ramona.brunner@my.jcu.edu.au), MG (mila.grinblat@my.jcu.edu.au), AM (aurelie.moya@gmail.com), DH (david.hayward@anu.edu.au), BL (viso3841@gmail.com), EB (eldon.ball@anu.edu.au), IC (ira.cooke@jcu.edu.au), DM (david.miller@jcu.edu.au)

Corresponding authors: EB and DM

Keywords: Maternal-zygotic transition, juvenile-adult transition, metamorphosis, coral development, larval settlement

Ethics and integrity statement: Our work does not require ethics approval, but all work involving the biota of the Great Barrier Reef requires approval by The Great Barrier Reef Marine Park Authority (GBRMPA) which rigorously assesses research plans before issuing appropriate permits and carries out routine surveillance. The work described here was conducted under GBRMPA permit G13/36196.1. The authors were all directly involved in the work and all have been consulted on draft and final versions of the manuscript. All analyses have been subject to scrutiny by other authors and can be confirmed using the web-based tool that we have released (see below).

Data availability: The transcriptome data and web-based browser reported here are available at https://amil2dev.mmb.group/. The source code is available at https://github.com/iracooke/amil2_dev.

Funding statement: This work was supported by grant numbers DP170104734, FS110200046 and CE14100020 from the Australian Research Council

The authors declare no conflicts of interest

Ethics approval, patient consent and clinical trial registration are not required for this work

Permission to reproduce material from other sources: Permission has been obtained to reproduce parts of Figure 5 from a previous publication by our group (Hayward et al. 2004). Smaller parts of other figures from our previous publications have been included in other figures, as cited in their captions.

Abstract

Background

Given the ecological importance of reef-building corals (Scleractinia), it is perhaps surprising that the molecular mechanisms underlying many of the morphological and metabolic changes during their development remain unclear. In part, this is due to the lack of a comprehensive transcriptomic dataset for any coral. A second challenge in the analysis of such non-model developmental datasets is that the volume of data often complicates its interpretation.

Results

To overcome these limitations, we profiled gene expression in *Acropora millepora* across 26 life stages from unfertilised eggs to juvenile polyps and developed an interactive online tool based on the R-application Shiny to simultaneously visualise changes in the expression of large numbers of genes. As expected, major transcriptomic changes (transitions) occurred during gastrulation and the acquisition of competence. Surprisingly, however, settlement triggered by using the natural inducer CCA did not immediately lead to major changes in gene expression, but a major transition involving many genes was observed 3 - 6 hours after settlement induction.

Conclusions

We hope that providing access to this extensive developmental transcriptome dataset and software to facilitate its analysis will expedite a better understanding of the changes that occur during coral development. The online tool is available at https://amil-deview.mmb.guide.

Background

Broadcast spawning corals, such as *Acropora*, release buoyant eggs and sperm and fertilisation occurs in the water column. The early developmental stages are planktonic, ultimately reaching a motile stage known as a planula larva which becomes “competent” – that is, it becomes capable of settlement and metamorphosis - after a period of development of variable duration (Figure 1). Competence is marked by a change in behaviour, from horizontal swimming to swimming into the substratum and testing it for chemical cues. In nature, the settlement of competent larvae generally involves selection of appropriate sites, based on perception of a range of cues that include small molecules, at least some of which are produced by bacteria associated with substrate biofilms and algae (e.g. Tebben et al. 2015; Siboni et al. 2020; Quinlan et al. 2023; Turnlund et al. 2025). The quality and nature of available light also plays a part in settlement site selection in the case of many reef-building corals (Mason and Cohen, 2012; Strader et al. 2015; Mason et al. 2023).

Various aspects of early coral development have previously been studied (Table 1), with the initial focus being characterisation of individual genes homologous to those playing key developmental roles in bilaterians (Ball et al. 2002; Hayward et al. 2002; Ball et al. 2004; Hayward et al. 2004). The first larger scale analyses were based on microarrays (Grasso et al. 2008; Reyes-Bermudez et al. 2009; Grasso et al. 2011), 454 GSFlx sequencing (Meyer et al. 2009), SOLiD sequencing (Meyer et al. 2011) or subtractive hybridisation (Hayward et al. 2011). More recent studies have used high-throughput DNA sequencing technologies to characterise specific developmental stages (Summarised in Table 1). Much of this work has focussed on members of the

Acroporidae (genera Acropora and Montipora), with sampling regimes designed to address specific questions. For example, Chille et al. (2021) concentrated on gene expression changes *in Montipora digitata* during the maternal/zygotic transition (MZT). However, two recent developmental studies on *M. digitata* have gone beyond transcriptomics and are particularly relevant to the work presented here. He et al. (2024) combined spatial gene expression data with a comprehensive temporal dataset to study the segmentation of the gastric cavity, and Huffmeyer et al. (2025) supplemented transcriptomic data with metabolomic analyses to investigate the nutritional shift from maternal lipids to symbiont photosynthates in this vertically transmitting coral. Much higher cellular resolution expression datasets are becoming available for scleractinians (Levy et al. 2021; Gilbert et al. 2024; Ramon-Mateu et al. 2025), but so far these have been limited to a few developmental stages.

To address the need for a comprehensive transcriptomic dataset, we profiled gene expression of *Acropora millepora* across 26 life stages from fertilised eggs to juvenile polyps and developed an interactive online tool based on the Shiny web framework to visualise changes in the expression of groups of genes. We present an overview of the data, focussing on major transitions in gene expression and on processes not previously investigated, but hope that further exploration of the dataset via the website facilitates progress towards solutions for the crises currently faced by coral reefs worldwide. Our study also reveals the importance of combining spatial expression data, as revealed by in situ hybridisation, with the data obtained by RNAseq, in order to better understand gene function.

130 **Materials and Methods**

131

132 Colonies of *Acropora millepora* were collected at Orpheus Island, Queensland,
133 Australia, (18.6141° S, 146.4892° E) under GBRMPA permit G13/36196.1 shortly
134 before they spawned at approximately 9pm on 21 November 2013. The samples
135 sequenced were the result of crosses between two colonies and were raised in three
136 separate flow-through tanks to control for tank effects.

137

138 Material was collected from 26 different time points of which 14 were sampled before
139 and 12 after settlement induction. Pre-settlement, samples were collected from
140 unfertilised eggs, at 5 hours post-fertilisation (hpf; 16-64 cell stages), 13hpf
141 (prawnchip), 18hpf, 23hpf, 29hpf, 35hpf, 40hpf (sphere, some swimming), 45hpf
142 (spheres, all swimming), 57hpf, 69hpf, 81hpf (planulae prior to the searching phase),
143 93hpf (searching planulae) and at 133hpf. At these stages, approx. 500 embryos per
144 replicate (n=3) and cross (n = 2) were immersed in 2 mL ethanol (100%). This
145 caused them to sink to the tube bottom, so that the overlying liquid was removed
146 before tubes were snap-frozen in liquid nitrogen.
147 To assess settlement competency, between 69 and 93hpf, aliquots of planulae were
148 exposed (independently) to either ethanolic extracts of the crustose coralline alga
149 (CCA) *Porolithon onkodes*, (kindly provided by Mikhail V. Matz) or the neuropeptide
150 Hym-248, both of which are known to induce settlement of *Acropora* planulae. At the
151 93 hpf stage 100% of planulae rapidly responded to the CCA extract by undergoing
152 settlement followed by metamorphosis, hence the settlement-induced stages used
153 for RNAseq were derived from planulae exposed to this inducer. Post-settlement
154 samples were collected by stocking 144 petri dishes (2 replicates x 3 larval tanks x 2

155 crosses x 12 time points) with respectively 100 larvae at the age of 133 h. Settlement
156 was induced with ethanolic CCA extract in all petri dishes at the same time. At the
157 respective sampling times of 15 minutes after induction (mpi), 30mpi, 1, 2, 3, 6, 9,
158 12, 18, 24, 48 and 72 hours post induction (hpi), unattached larvae were transferred
159 into tubes, and attached settlers were snap-frozen on petri-dishes using liquid
160 nitrogen after excess seawater was decanted. Sample tubes and petri dishes were
161 taken to James Cook University, (Townsville, Australia) in dry-ice, and stored at -
162 80°C until further processing.
163
164 Frozen samples in the plates were submerged in RNAlater-ICE and allowed to thaw
165 overnight at -20°C. Once thawed, RNAlater-ICE was removed and replaced by 2ml
166 of *mir*Vana™ homogenisation buffer. Polyps were gently scraped off the plate with a
167 sterilized scalpel in the homogenisation buffer and transferred into a 2ml tube for
168 immediate processing.
169 For both pre- and post-settlement samples, total RNA was extracted using
170 the *mir*Vana™ miRNA Isolation Kit (Ambion) according to the manufacturer's
171 instructions. RNA quantity and quality were assessed using a NanoDrop ND-1000
172 spectrometer and denaturing gel electrophoresis using standard methods (Russell &
173 Sambrook 2001) before being shipped on dry-ice to AGRF in Brisbane for Hi-Seq
174 paired-end sequencing.
175
176 RNA sequencing data for all samples was first checked using a Nextflow (Di
177 Tommaso et al. 2017) pipeline https://github.com/marine-omics/moqc. This pipeline
178 includes fastqc (v0.11.5; https://www.bioinformatics.babraham.ac.uk/projects/fastqc/)
179 to check raw read quality, and read-level taxonomic classification via krakenuniq

180 (v1.0.2 ; Breitwieser, Baker and Salzberg, 2018) to determine the dominant symbiont
181 genus and check for bacterial or eukaryotic contaminants. All samples were
182 dominated by reads attributable to the coral host but also contained a small fraction
183 (0.5-2%) from Symbiodiniaceae, of which *Durusdinium* was the dominant genus. No
184 samples were flagged as having low quality base calls, excessive adapter
185 contamination or high levels of potential contaminants (eg bacteria).
186
187 After confirming the overall quality of read data for all samples, reads were trimmed
188 using fastp (Chen, Zhou, Chen and Gu, 2018) to remove adapters and low-quality
189 sequences. Trimmed reads were then aligned to a combined reference database
190 consisting of all *Acropora millepora* transcripts predicted from gene models along
191 with the transcriptome of an unnamed *Durusdinium* species (Shoguchi et al. 2021).
192 Alignment was performed using Bowtie2 (v2.5.0; Langmead and Salzberg, 2012) as
193 part of RSEM (v1.3.3; Li, B., Dewey, C.N., 2011) and used to produce transcript level
194 counts for each sample. All of these steps were run using a Nextflow pipeline
195 https://github.com/marine-omics/morp.
196
197 Transcript counts produced by RSEM were imported into R and processed using the
198 variance stabilising transform function in DESeq2 (vv1.38.3; Love, Huber and
199 Anders, 2014) to produce values on a log2 scale for visualisation.
200
201 Functional annotations for *Acropora millepora* transcripts were obtained using a
202 nextflow pipeline (https://github.com/marine-omics/moat) that is primarily based
203 around identifying homologous proteins in Swissprot (downloaded December 2022)
204 via blastp and blastx (NCBI Blast+ v 2.13.0). In this process, any protein with an

evalue less than 1e-5 is considered a hit and the best hit is used to lookup Gene Ontology ID's and a protein name from the Swissprot database. In addition, transcripts were annotated with conserved domains, gene family membership and an alternative Gene Ontology ID inferred using Interproscan (v5.59-91.0; Jones et al. 2014).

Principal component analysis (PCA) was conducted using the prcomp function of the stats package in R with vst normalised counts.

Weighted gene co-expression network analysis (WGCNA) was conducted with normalised data that were filtered for genes with excessive number of missing values or zero-variance using the goodSamplesGenes function of the WGCNA package (Langfelder & Horvath, 2008). The samples were clustered using the function hclust of the stats package (R Core Team, 2024) to detect outliers. One sample collected 3 hpi was removed from the analysis. To determine groups of genes +(modules) with correlated developmental gene expression profiles, a weighted gene co-expression network was constructed blockwise using the function blockwiseModules with a maximum block size of 18000 genes, a minimal module size of 18 and a mergeCutHeight set to 0.25. A signed, scale-free topological overlap matrix for each block was created by choosing a soft threshold power of 12 and a biweight midcorrelation.

To facilitate reuse and rapid exploration of the *Acropora millepora* developmental transcriptome we created an interactive web application using the shiny framework (https://shiny.posit.co/) . This application is hosted on servers provided by the Australian Research Data Commons Nectar Research Cloud to ensure that it is scalable and highly available for long-term use. Users can access the web

application directly at https://amil2dev.mmb.group/ or obtain its source code and the underlying data from our github repository (https://github.com/iracooke/amil2_dev). The application is designed to facilitate access to developmental expression profiles for individual genes or groups of genes. Users can define genes of interest in two ways by either conducting a BLAST search of a sequence or by directly searching for genes with metadata matching a set of gene identifiers, Pfam domains, GO term IDs or text as part of the protein name. Once a list of genes has been identified, the corresponding normalised gene expression data is rapidly retrieved from an sqlite relational database and used to generate an interactive display. When the number of genes is small (default <10) each gene is displayed using a separate line plot generated by the R package ggplot2 (Wickham, 2016) so that detailed changes in the expression of each gene can be carefully inspected. For larger numbers of genes (default>=10) we assume that the user is more interested in broad patterns among genes and the display changes to an interactive heatmap generated with the R package InteractiveComplexHeatmap (Gu and Hübschmann, 2022). In both cases a list of genes with annotation information is also displayed and users can select rows in this table to adjust which genes are displayed in the main display. Comprehensive data and code exporting functions are also provided so that users can easily export both data and R code to reproduce the plots seen in the app to allow further customisation by the user.

255 **Results**

256

257 **Major transcriptional transitions visualised using DEView**

258 During the development of *A. millepora*, the period immediately following fertilisation
259 (0 – 5h) was characterised by rapid rounds of cell division (Figure. 1) accompanied
260 by relatively limited changes in gene expression (Figure. 2), implying that this phase
261 is driven largely by maternal mRNAs and proteins. After that time more extensive
262 changes in gene expression occurred resulting in resolvable PCA clusters. After
263 completion of gastrulation at 35hpf, embryos were spherical and became motile at
264 45hpf. Elongation from pear- (57hpf) to spindle-shaped larvae (69hpf) resulted in
265 planulae that were not searching at 81hpf but were probing the environment for
266 appropriate settlement sites at 93hpf, by which time they were competent to settle
267 (Figure. 1). At 133hpf, settlement was induced with ethanolic CCA extract but the
268 133hpf transcriptome data represent the untreated state. Settlement induction
269 caused larvae to further elongate at 15mpi before forming disc-like shapes by
270 contracting along the oral-aboral axis. Most larvae were metamorphosed at 2hpi and
271 by 3hpi 100% of larvae had initiated metamorphosis characterised by a six-fold
272 symmetry around an oral pore in the centre. Whereas transcriptome data for the 0-
273 3hpi stages clustered with those for late planula stages, data for 6 – 72hpi stages
274 formed a discrete and well-resolved cluster (Figure. 2) during which metamorphosing
275 polyps developed a 12-fold symmetry and formed tentacles around the oral opening.
276 The polyp initiates calcification at the former aboral part, which becomes the
277 calicoblastic ectoderm.

278

Differential gene expression analysis (Figure 3) clearly highlights that, in addition to the expected early (13-29hpf) transcriptional events corresponding to zygotic genome activation, major transitions in gene expression also occurred at 81-93hpf and 3-6hpi. The construction of weighted gene co-expression networks (WGCNA; Langfelder & Horvath (2008), which group modules of genes according to correlation in their expression patterns, also support a 3-transition hypothesis of early coral development (Supplementary Figure 1). Whilst such analyses are informative with respect to the major transitions in development, they are less useful for exploration of the expression patterns of subsets of genes in terms of structure or function according to Pfam or Gene Ontology (GO) IDs. To facilitate these latter kinds of analyses, a software tool based on the Shiny web framework (https://shiny.posit.co/) was developed (https://amil2dev.mmb.group/).

One powerful feature of the new software tool is that it allows the simultaneous visualisation of developmental gene expression patterns from a subset of genes defined by gene identifiers, Pfam domains or GO terms. These subsets can be selected for further analyses and comparison based on morphology, behaviour, or gene expression patterns, such as occur during gastrulation and settlement.

Whilst early zygotic gene expression accompanied gastrulation, the major transition at 81-93hpf is likely to correspond to larval competence which is the preparation for settlement and metamorphosis. Both of these transitions have previously received considerable attention (e.g. Hayward et al. 2011; Grasso et al. 2011; Strader et al. 2018). Metamorphosis was underway by 3hpi and was followed by changes in the expression of large numbers of genes (Figure 2, Figure 3). This post-settlement

304 change in the expression patterns of many coral genes has previously received only
305 limited attention (Ishii et al. 2022) and therefore merited closer examination. In what
306 follows we have proceeded chronologically, with a particular focus on processes and
307 classes of genes not discussed in previous studies.
308

309 **Maternal transcripts and the earliest transcriptional events**

310 As in most animals, early post-fertilisation development in corals consists of rapid
311 cell division during which the maternal cytoplasm is serially subdivided (reviewed in
312 Ball et al. 2021), and the transcripts required to facilitate these events are largely
313 provided maternally. Extensive zygotic gene expression appears to be initiated
314 leading into gastrulation (i.e. around 13h post-fertilisation; Figure 1, Figure 2)
315 corresponding to the “prawn-chip” morphology.
316

317 Rapid rounds of cell division during early development require that replication occurs
318 quickly, generating a need for core histone proteins in large amounts to form the
319 H2A/H2B and H3/H4 dimers that constitute the nucleosomes responsible for
320 packaging the DNA into chromatin. As in *Hydractinia* (*Klyxum*) *echinata* (Ayers et al.
321 2023), histone mRNAs are amongst both the most abundant maternal transcripts
322 and earliest expressed zygotic genes in *Acropora* (Figure 4A). Note, however, that
323 the early zygotic (canonical) histone transcript profile is likely to be dominated by the
324 replication-coupled types.
325 Transcripts encoding the core histones H2B, H3 and H4 are particularly abundant in
326 the *Acropora* maternal mRNA complement (Figure 4A), and the zygotic expression
327 of these histone types began early at the onset of gastrulation with a peak at 13-
328 18hpf for H3, H4 and H2B (XP_044167100.1, XP_044175889.1) (Figure 4A).

329 Curiously, however, canonical H2A mRNA was not maternally provisioned at
330 significant levels, instead, one of two H2A.X homologs (H2A.X2; XP_029204486.1)
331 and, to a lesser extent, H2A.V (H2A.F/Z; XP_029205888.1) transcripts were
332 maternal. Levels of mRNA encoding maternal H2A.X in the unfertilised eggs were
333 very high but fell dramatically after 13hpf as zygotic expression of canonical H2A
334 began (e.g. XP_044167969.1), and H2A.X transcripts were essentially absent by
335 29hpf (Figure 4A).
336
337 Gastrulation is characterised by large scale activation of zygotic genes, requiring
338 extensive chromatin modification. Consistent with this, high levels of mRNAs
339 encoding homologs of the histone acetyltransferase (HAT) KAT6A
340 (XP_029189526.2) and SETD2 (XP_029190384.2) were provided maternally (Figure
341 4B). The latter is the only histone methyltransferase capable of generating the
342 H3K36me3 modification essential for transcriptional activation (Michail et al. 2025).
343 Note that both of these genes were reactivated during the post-settlement transition
344 discussed below.
345
346 **The MZT occurring at gastrulation marks the first major developmental**
347 **transition**
348 To date, the process of gastrulation has been the most extensively studied aspect of
349 developmental gene expression in both corals and *Nematostella* (Technau, 2020). In
350 situ hybridisation analyses have shown that orthologs of several key developmental
351 regulators from bilaterians are temporally and spatially expressed in *A. millepora*
352 consistent with conservation of function. Examples of these include *snail* (Hayward
353 et al. 2004), *brachyury* (Hayward et al. 2015; Yasuoka et al. 2016), *forkhead*

354 (Hayward et al. 2015) and *dpp/bmp4* (Hayward et al. 2002) (Supplementary Figure
355 2).
356 With the sole exception of *Pavona*, all complex corals examined to date go through a
357 "prawn chip" stage of early development that corresponds to the early gastrula
358 (Okubo et al. 2013 and references cited there; Okubo et al. 2016). At this stage, a
359 homolog of *Drosophila snail* (XP_029185944.1) was expressed in the presumptive
360 mesendoderm (Hayward et al. 2004). As *snail*-expressing cells are undergoing an
361 epithelial-mesenchymal transition (EMT), one of several *Acropora* genes related to
362 *Drosophila* aristaless (XP_044163657.1/XP_029193169.1) was expressed
363 throughout the presumptive ectoderm (Figure 5). Hence these two genes effectively
364 demarcate the two primary tissue layers of *Acropora* during gastrulation.
365
366 **The late planula transition corresponds to the acquisition of larval competence**
367 During the period 81-93hpf, many genes show strong down-regulation, but this is
368 immediately followed by the up-regulation of an even larger number of genes during
369 the 93-133hpf time window (Figure 3).
370
371 These timepoints correspond to the acquisition of settlement competence and when
372 *Acropora* larvae are searching for cues that identify appropriate settlement sites (eg.
373 Tebben et al. 2015, Siboni et al. 2020, Quinlan et al. 2023, Turnlund et al. 2025) by
374 swimming along the substratum to periodically sample it with the aboral end.
375
376 Settlement involves the aboral larval ectoderm making contact with substratum,
377 which is likely coated with attractive and potentially hostile bacteria, and among the
378 upregulated genes a number encode proteins with known or suspected antimicrobial

379 properties. Among them are for example AmAMP1 (Mason et al. 2021;
380 XP_029188806.1), the MAC-Perforin protein apextrin (Miller et al. 2007; Hayward et
381 al. 2011; XP_044181104.1) and the quorum quenching enzyme AmNtNH1 (Mason
382 et al. 2024; XP_029207486.1). Figure 6 summarises developmental expression data
383 for these three genes.
384
385 This study also provides the most direct evidence to date in support of Hadfield's
386 hypothesis (Hadfield, 2000) that coral larvae are primed for settlement and
387 metamorphosis via prior gene expression. Whilst several thousands of genes are up
388 or down regulated during the onset of competency (81- 133hpf), settlement and the
389 initiation of metamorphosis largely happen without changes in gene expression
390 (Figure 3). With the caveat that datasets and technologies were much less
391 sophisticated than those presently available, Grasso et al. (2011) came to the same
392 conclusion for *A millepora* based on microarrays, as did Strader et al. (2018)
393 indirectly by correlating expression data for competent larvae with settlement-
394 induced larvae from Meyer et al. (2011).
395
396 **The post-settlement gene expression transition resembles an MZT in terms of**
397 **scale and involvement of some specific components**
398 The scale of the post-settlement transition between 3-6hpi resembles that typical of
399 an MZT. In *Acropora*, we estimate that approximately 20% of mRNAs undergo at
400 least a two-fold change in expression level (i.e. are either up- or down-regulated over
401 the 3-6hpi time window). By comparison, in the zebrafish approximately 25% of
402 maternal transcripts are cleared during the MZT (Mishima and Tomari, 2017) and the
403 corresponding number for *Caenorhabditis* is around 33% (Baugh et al. 2003). Many

404 of the mRNAs up-regulated over the 3-6hpi time window in *Acropora* coded for
405 transcription factors or other regulatory proteins involved in chromatin modifications
406 and mRNA processing.
407
408
409 **Chromatin modification during early development and at the post-settlement**
410 **transcriptional transition**
411 Major changes in gene expression patterns also generally involve chromatin
412 modification events, so histone modification and DNA methylation changes are to be
413 expected. Homologs of a number of key chromatin modifiers are differentially
414 expressed at the 3-6hpi transition.
415
416 In many animals, homologs of TET (ten-eleven translocation) are the primary agents
417 responsible for demethylation of 5-methylcytosine residues (MeCpG) in DNA and are
418 required for gene activation (Mohr et al. 2011; Wu and Zhang 2017; Jessop et al.
419 2018). As well as a transient earlier (5hpf) window of expression leading into the
420 early MZT, the *Acropora TET* homolog (XP_029179484.2) was strongly upregulated
421 at the 6hpi time point (Figure 7A), suggesting a role for the *Acropora* TET homolog in
422 relieving repression by erasing pre-existing MeCpG marks.
423
424 DNA methylation is generally associated with repression of transcription, the
425 enzymes associated with maintenance and *de novo* DNA methylation being the DNA
426 methyltransferases DNMT1 and DNMT3, respectively.
427 In the case of *Acropora*, mRNAs encoding the DNA methylases DNMT1
428 (XP_029197815.2) and DNMT3a (XP_029213858.1) were maternally provided,

429 zygotic expression of DNMT1 being detected between 29hpf and 12hpi, despite
430 having faded by 81hpf. Both DNMTs were upregulated 12 to 18hpi (Figure 7A)
431 expression of DNMT3a appeared to be stronger than that of DNMT1 (Figure.7A)
432
433 **mRNA degradation during major transitions in development**
434 Perhaps the major characteristic of MZTs is the elimination of a subset of maternally
435 provided mRNAs (often a major proportion) to facilitate the transition to the zygotic
436 developmental program. The mRNA elimination process employs a range of
437 mechanisms to destabilise or degrade transcripts, but some conserved players have
438 been identified during major transitions, including homologs of the *Drosophila* genes
439 *Pumilio* (Gerber et al. 2006; Rabani et al. 2017) and *Smaug* (Chen et al. 2014) as
440 well as the *Caenorhabditis* protein TRIM71/LIN41 (Spike et al. 2022).
441
442 Transcripts annotated as *Pumilio* (XP_029180703.2 and XP_029180704.2) were
443 maternally provided but were essentially cleared after 29hpf, whereas a distinct
444 Pumilio homolog (XP_044164192.1) was not represented in the maternal mRNA
445 complement but was expressed from 18hpf (Figure 7B). Each of these Pumilio
446 homologs was up-regulated over the 3-6hpi time window after earlier periods of
447 activity.
448
449 Members of the Smaug/SAMD4 family of proteins are highly conserved (yeast to
450 man) regulators of mRNA stability and transcriptional repressors that act in
451 development by binding to specific RNA sequence motifs. Smaug proteins have
452 been implicated in erasing maternal transcripts during the MZT in the early
453 development of diverse animals (Chen et al. 2014; Chille et al. 2021) implying that

454 the Smaug homolog fulfills a similar function in the early development (around 4hpf)
455 of the coral *Montipora capitata*. Although an early “flutter” of Smaug expression,
456 possibly corresponding to that reported in *Montipora* (Chille et al. 2021), was
457 observed in *Acropora* at 5hpf, Smaug (XP_029197445.1) was predominantly
458 expressed at 15mpi - 6hpi (peak) (Figure 7B). A second transcript annotated as
459 Smaug (XP_044163536.1) was mildly up-regulated at 13-18hpf.
460
461 Members of the TRIM71/LIN41 family of E-3 ubiquitin ligases are highly conserved
462 RNA-binding proteins (Aviv et al. 2003) that facilitate major developmental transitions
463 in *Caenorhabditis* (Spike et al. 2022). At least one member of this gene family
464 (XP_029198843.2/XP_029198844.2) is up-regulated at the 3-6hpi time point during
465 *Acropora* development, suggesting that they may also be involved in protein
466 clearance at the 3-6hpi transition.
467
468 **Small RNA processing pathway components**
469 Small RNAs (miRNAs, siRNAs and piRNAs) have important regulatory functions
470 during the development of many bilaterians (Bartel, 2004) and this is likely to also be
471 the case in *Acropora* given that at least some components of the miRNA processing
472 pathway are known to be differentially expressed during the development of
473 *Nematostella* (Praher et al. 2017). In cnidarians, the biogenesis of miRNAs follows a
474 plant-like pathway (Moran et al. 2017), but homologs of some of the enzymes in the
475 animal miRNA processing system are also present and may also participate in
476 miRNA synthesis.

477 To address the possibility of miRNAs participating in gene regulation during early
478 coral development, the expression of components of both the plant and animal
479 processing pathways was investigated (Figure. 8).
480
481 Some of the small RNA processing pathway components were provided maternally,
482 levels of transcripts annotated as Dicer-like (XP_029197160.2) and the HEN1
483 methyltransferase (HEN1MT; XP_029185006.2) being present at high levels. In
484 cnidarians, HEN1 is responsible for methylation of the 3'-ends of both miRNAs and
485 piRNAs, resulting in their stabilisation. The observed upregulation of HEN1 at 93hpf
486 (Figure. 8) is consistent with a role in metamorphosis of *Acropora* larvae, as in
487 *Nematostella* (Modepalli et al. 2018).
488 The maternal mRNA repertoire also included an Argonaute homolog
489 (XP_044181068.1) and a *Acropora* Piwi-like protein (XP_029187700.2/
490 XP_029187701.2) (Figure. 8) that likely function together in transposon silencing
491 during early development, as in *Nematostella* (Fridrich et al. 2020; Bamberger et al.
492 2022). The high abundance of mRNA encoding a homolog of the Maelstrom protein
493 (XP_044166539.1) also attests to the importance of the piRNA-mediated transposon
494 silencing pathway (Matsumoto et al. 2015; Sato and Siomi, 2015) during the earliest
495 stages of coral development.
496 Although not maternal, other miRNA pathway components were expressed very
497 early in development (Figure 8). Transcripts annotated as DGCR8/Pasha
498 (XP_029194207.2) and SRRT/Serrate (XP_044181962.1) were first detected as the
499 early embryo was going into gastrulation at about 13hpf. For both of these genes,
500 other transcripts carrying the same annotation appeared to be expressed during
501 different stages of development. In the case of SRRT/Serrate, XP_044181962.1 is

502 expressed in the early gastrula but most heavily after the initiation of metamorphosis
503 (6hpi). A second isoform/splice variant (XP_044181963.1) was most highly
504 expressed very early in the settlement process (15mpi - 2hpi) – i.e. prior to what Ishii
505 et al. (2022) referred to as the “point of no return”.
506 Similarly, the DGCR8/Pasha paralogs or splice variants XP_029194207.2 and
507 XP_029194208.2 seem to have distinct expression profiles during development
508 (data not shown).
509 In addition to the maternal Piwi-like mRNA (XP_029187700.2/ XP_029187701.2), a
510 second (non-maternal) Piwi (XP_044168784.1/ XP_044168785.1/ XP_044168786.1)
511 was expressed from the early gastrula stage, peaking in expression as the maternal
512 type was fading.
513
514 **Discussion**
515
516 The study of early coral (*A. millepora)* development presented here was based on
517 gene expression profiles obtained for 26 developmental stages spanning the period
518 between unfertilised eggs and 3-day-old primary polyps. Downstream analyses via a
519 DEView app revealed three major transcriptomic transitions - the maternal-zygotic
520 transition, the acquisition of competence by planulae (93-133hpf) and a post-
521 settlement transition (3-6hpi) that has not previously received significant attention.
522 This latter novel transition in gene expression resembled an MZT in terms of scale
523 and the involvement of some key genes. In addition to regulatory genes involved in
524 chromatin modification and RNA processing, we focused here on genes likely to
525 have protective roles, specifically those potentially involved in photoprotection, anti-
526 microbial activity and transposon silencing.

527

528 In many animals, mRNAs encoding canonical histones (including H2A) as well as the
529 corresponding proteins are provided maternally at sufficient levels to support the
530 earliest cell division events. To our knowledge, finding that in *Acropora*, an mRNA
531 encoding one H2A.X variant (H2A.XII) replaced that for canonical H2A in the eggs is
532 novel. H2A.X is a histone variant whose best-defined role is in DNA repair (reviewed
533 in Lorkovic and Berger, 2017; Herchenröther et al. 2023). It is closely related to
534 canonical H2A but distinguished from it by the presence of a characteristic C-
535 terminal sequence extension that includes a serine residue subject to
536 phosphorylation generating the gammaH2A.X form which is required for binding at
537 double-stranded DNA breaks (Osakabe and Molaro, 2023). The enzymes
538 responsible for this phosphorylation of H2A.X are Phosphoinositide-3-Kinase-related
539 protein kinases (PIKKs), and at least one PIKK-related protein kinase
540 (XP_029200091.2) is provided maternally in *Acropora*, though it is unclear whether
541 H2A.X is a substrate for this activity.

542

543 Whilst most coral spawning occurs during the night, the gamete bundles (or eggs)
544 released are buoyant so that the earliest developmental events occur near the
545 water's surface. In the present study, *Acropora* larvae became motile 40-45hpf by
546 which time they would have been exposed to two days of direct sunlight. Early
547 developmental stages of corals therefore face exposure to UV radiation at levels that
548 can cause DNA damage, and H2A.X2 mRNA may be maternally provided at high
549 levels to facilitate maintenance of DNA integrity through the earliest developmental
550 stages. Chille et al. (2021) noted high representation of GO terms associated with
551 DNA repair in the maternal mRNA complement of *Montipora* but did not identify

552 specific genes/proteins. GFP-related proteins are also thought to be involved in DNA
553 protection in corals (Salih et al. 2000; Palmer et al. 2009; Bou-Abdallah et al. 2006;
554 Clarke et al. 2024) and, consistent with the study of Strader et al. (2018), at least four
555 distinct types are expressed during the larval and early polyp stages. Although
556 mRNAs encoding GFPs did not appear to be maternally provided at significant
557 levels, the pigmentation of the eggs of many coral species is consistent with the idea
558 of maternal provision of photoprotective agents that likely include GFP-related
559 proteins, which are known to be long-lived.
560 Note that in *Acropora* there is a second H2A.X-like gene (H2A.X1; XP_029200990.1
561 - annotated as H2A-like) that is expressed only at relatively low levels during early
562 development. This second H2A.X isoform (XP_029200990.1) has an N-terminal
563 tyrosine residue replacing the phenylalanine in XP_029204486.1 and has close
564 homologs in *Hydra* (CDG71330.1; 86.47% protein identity to *Acropora*) and
565 *Hydractinia* (now *Klyxum*; AOF43153.1; 87.02% identity) and, like those, is
566 presumed to be the main isoform expressed during post-larval life. In *Hydractinia*
567 (now *Klyxum*) *echinata*, the H2A.X variant AOF43152.1 is expressed specifically in
568 female germ cells along with canonical histone H2A (Torok et al. 2016) and may be
569 functionally equivalent to the maternally provided *Acropora* H2A.X homolog
570 XP_029204486.1 (protein sequence identity of 68.15%).
571

572 **Comparisons with published studies of coral development**

573 The most interesting observation made here was the extent and nature of the post-
574 settlement transcriptional transition observed at 3-6hpi. This major change in gene
575 expression is more apparent than in previous studies which either did not include
576 post-settlement stages (Strader et al. 2018; Chille et al. 2021) or sampled sparsely

pre-settlement (Huffmeyer et al. 2025) or after settlement induction (Ishii et al. 2022, Meyer et al. 2011) (Table 1). Furthermore, comparisons between the work presented here and previously published papers in this field (Table 1) are complicated due to the diversity of species studied, differing temperatures during development, differing sampling points and differing inducers used to trigger settlement and metamorphosis.

Development has been studied primarily in members of the three coral genera *Acropora, Montipora* and *Porites*. Whilst these are all members of the “superfamily” Complexa, and the first two belong to the same coral family (Acroporidae), both *Montipora* and *Porites* spp. maternally transmit Symbiodiniaceae whereas *Acropora* spp. acquire their symbionts from the environment during early life.

Chille et al. (2021) focussed on MZT and therefore studied gene expression changes during development of *Montipora capitata* from unfertilised egg to planula in addition to adults. Some of their MZT results are consistent with those presented here for *Acropora*, for example the expression of Smaug (Figure 7B) and Brachyury (Supplementary Figure 2) in prawn chip and early gastrula.
However, the rate of development of *M. capitata* observed was apparently slower than that of *Acropora*. *Montipora capitata* reached the late gastrula stage after 1.5 days, whereas *Acropora* generally reaches the corresponding stage earlier (around 30hpf). This demonstrates the complication of relating developmental stages across datasets where interspecific differences can be compounded by the presence/absence of maternal photosymbionts and different rearing temperatures, as higher temperatures accelerate development. Using GO-term data, Huffmeyer et

al. (2025) recognised three distinct (but overlapping) phases of gene expression during the early development of *Montipora*.

Since morphology reflects changes in gene expression, we have found that comparisons of gene expression based on morphology are more meaningful than those based on time, even in the single species *A millepora*. The post-settlement transition remained unexplored in the study of Chille et al. (2021) since the focus on MZT did not require the sampling of post-settlement stages. The 3-6hpi gene expression transition observed here may correspond to what Ishii et al. (2022) refer to in their study as “the point of no return” (PNR), a point in post-settlement development after which reversibility by aborting settlement and returning to the motile phase is lost. Whilst the Ishii et al. (2022) paper focussed on gene expression changes between three time points during metamorphosis in *Acropora*, comparison between their results and those presented here is complicated by the differing triggers used to drive the process. For *Acropora* spp., external exposure of competent larvae to the *Hydra* GLWamide (Hym-248), directly triggers metamorphosis, essentially overriding the need for external settlement cues (Iwao et al. 2002; Grasso et al. 2011; Attenborough et al. 2019). Whilst Ishii et al. (2022) induced metamorphosis using Hym-248, the study described here triggered settlement by addition of CCA extract, which induces searching behaviour rather than directly driving metamorphosis (Grasso et al. 2011). Hence it is not possible to directly compare developmental timing between these two studies. The 1hpi and 6hpi time points in the Ishii paper are likely to correspond to later time points in the present study, as the duration of the settlement period must be several hours longer when using CCA extract compared to Hym-248. The PNR inferred by Ishii as occurring at 4hpi may correspond to the 3-6h transition identified in the present work

627 but note that rates of larval development can be strongly influenced by temperature.
628 The differences in gene expression between untreated (0 hr) and 1 hour after
629 induction described in the Ishii et al. paper are therefore likely to encompass a
630 number of distinct time points in our study, so subtle transcriptional changes
631 occurring during the searching and very early settlement phases were presumably
632 not noted by Ishii et al. (2022).
633

634 **The post-settlement transition – a cnidarian equivalent of the *Caenorhabditis***
635 **"juvenile to adult" transition?**

636 In *Acropora*, the transition from larvae to recruits at 3-6hpi has several parallels to
637 maternal-zygotic transitions (Vastenhouw et al. 2019) regarding the removal of
638 earlier transcripts and genome activation appropriate for stages following the
639 transition. A precedent for such a later transition is provided by *Caenorhabditis*
640 *elegans*, where it is recognised as the juvenile to adult transition (Spike et al. 2022).
641

642 Above, the involvement of homologs of both *Drosophila* Smaug and Pumilio in the
643 mRNA clearance processes during MZT and the juvenile to adult transition at 3-6hpi
644 were highlighted. In addition, two transcripts with the same sequence
645 (XP_029198843.2 and XP_029198844.2) annotated as a member of the
646 TRIM71/LIN41 family of RNA-binding proteins were upregulated during the 3-6hpi
647 transition. Other members of this protein family have important roles in the regulation
648 of both oocyte to embryo (Spike et al. 2022) and juvenile to adult (Aeschimann et al.
649 2019) developmental transitions in *Caenorhabditis*. As in *Caenorhabditis* (Spike et al.
650 2022), this *Acropora* TRIM71/LIN41-related protein is likely to be involved in

651 regulatory changes at the 3-6hpi transition, and on this basis deserves further
652 exploration.
653
654 In addition, peaks in the expression of the DNA demethylase TET (Figure 7A) and of
655 SETD2 (XP_029190384.2) as well as homologs of the histone acetyltransferases
656 HAC5 (XP_029203404.2), KAT5 (XP_029179982.2) and KAT6A (XP_029189526.2)
657 (Figure 4B) around 3-6hpi imply extensive chromatin modification at that time.
658 Presumably, the corresponding proteins function in facilitating transcription of genes
659 required for early polyp development (e.g. He et al. 2024). Transcription factors (TF)
660 strongly up-regulated at the 3-6hpi time point include genes annotated as homologs
661 of FoxB1 (XP029196672.1) and FoxO (XP_029208531.2), Aristaless
662 (XP_029193170.1), Rax (XP_029193171.1), Meis2 (XP_029187327.1) and Otx
663 (XP_029190339.1), whilst homologs of Emx (XP_029211983.2), Pitx2
664 (XP_029179676.1) and Brn3C (XP_029213135.1) were simultaneously down-
665 regulated.
666
667 **Limitations: Heatmaps are useful but tell only part of the story**
668 A caveat in making inferences from heatmaps across developmental stages, and
669 more generally from whole-larvae overall expression levels, is that important subtle
670 changes may be missed. Particularly with transcription factors or other regulatory
671 molecules, low overall levels of expression may have major effects, especially when
672 restricted to subsets of cells. Consequently, interpreting developmental gene
673 expression requires not only temporal data, but also spatial information from the
674 application of in situ hybridisation or other techniques. This is clearly illustrated in

675 Supplementary Figure 2, which provides expression data for genes implicated in
676 conserved functions during gastrulation.
677 Whilst in situ hybridisation data show expression of these four genes in smaller
678 subsets of genes across all developmental stages between gastrulation and
679 metamorphosed recruit, the heatmaps show that the expression maxima occur post-
680 settlement rather than at gastrulation around 13 – 18hpf. Only a weaker peak in
681 expression of Brachyury at 13hpf corresponds to the early gastrulation window of
682 expression visualised via in situ hybridisation (Hayward et al. 2015). Consequently,
683 visualisations of spatial expression via in situ hybridisation are required to study the
684 function of selected genes. For example, whilst gene expression data presented in
685 the heatmap suggested functions post-settlement, ISH visualisations revealed that
686 temporal expression of an *Acropora* arx-related gene
687 (XP_044163657.1/XP_029193169.1) during gastrulation closely complements that of
688 snail (Figure 5). This *Acropora* sequence is referred to here as homeobrain, based
689 on its orthology with *Nematostella* XP_048583705.1 (Mazza et al. 2010). Snail and
690 homeobrain respectively demarcate the early mesendoderm and presumptive
691 ectoderm during gastrulation (Figure 5), but both are also expressed at higher levels
692 after settlement-induction where snail expression reaches its expression peak earlier
693 than in the case of homeobrain. Assuming these two genes fulfill similar function
694 during gastrulation and post-settlement, this suggests that a cell migration such as in
695 an epithelial-mesenchymal transition occurs during the initiation of metamorphosis.
696 The upper limit of expression in a heatmap is determined by the genes included in
697 that map so important changes in gene expression may not be as apparent as if the
698 gene was plotted against itself.
699

700 **Expression of the small RNA processing machinery during early development**

701 Despite deep evolutionary divergence between the sea anemones (Actiniaria) and
702 the coral/corallimorpharian lineage, many of the molecular processes underlying
703 early development in *Acropora* closely parallel those described in *Nematostella*
704 (Hayward et al. 2015), and this appears to extend to the machinery for processing
705 small RNAs (miRNAs and piRNAs). However, some differences were observed in
706 the timing of expression of several of genes implicated in small RNA processing.
707 Whilst mRNAs for Vasa1, Maelstrom and Piwi are provided maternally in *Acropora*
708 and *Nematostella*, Vasa2 (aka Vasa-like or DDX4) is also maternal in the coral
709 whereas the corresponding mRNA was not detected until around gastrulation in
710 *Nematostella* (Praher et al. 2017). Whether Dicer/DCL is maternal is unclear in the
711 case of *Nematostella*, whereas mRNA of the *Acropora* homolog of *Nematostella*
712 Dicer 2 (AGW15596.1), encoding XP_029197160.2, is abundant in *Acropora* eggs.
713 In summary, the preliminary data presented here indicate that all or most of the small
714 RNA processing machinery is either maternal or expressed very early in *Acropora*
715 development. It is therefore likely that, in addition to roles for some of these
716 components in transposon silencing, miRNAs are likely to have important regulatory
717 roles in the early development of *Acropora*.
718

719 **Heatmaps enable identification of candidate genes for key roles in early**
720 **development**

721 A major strength of the DEView app is that it provides a means of scanning classes
722 of genes individually or collectively for their expression patterns across early coral
723 development, allowing identification of candidates for roles in specific processes,
724 including settlement induction and the initiation of calcification. Whilst significant

725 progress has recently been made, we have as yet a relatively limited understanding
726 of the nature and recognition of settlement cues (Hadfield, 2011; Tran and Hadfield,
727 2012; Ball et al. 2021; Turnlund et al. 2025). The larvae of many corals select
728 appropriate settlement sites by detection of small molecules that either favour or
729 discourage settlement (e.g. Morse et al. 1988; Negri et al. 2001; Kitamura et al.
730 2007; Birrell et al. 2008; Kitamura et al. 2009; Tebben et al. 2015, Quinlan et al.
731 2023). Most likely the outcome reflects a combination of molecules acting as ligands
732 for specific receptors that are expressed in competent larvae and downregulated
733 after settlement and metamorphosis. Receptors that potentially could be involved in
734 settlement cue reception and downstream signalling pathways, respectively, are G-
735 Protein coupled receptors (GPCRs) and nuclear receptors. With the help of the
736 DEView app, search terms such as “G-protein coupled receptor” or specific Pfam
737 domains can be used as filters to search the developmental transcriptome to identify
738 genes that were upregulated at competency (i.e. 93hpf) consistent with their
739 potential involvement in settlement cue perception. Searching the *Acropora* data
740 using the terms PF00104 Ligand-binding domain of nuclear hormone receptor and
741 PF00105 Zinc finger, C4 type (two domains) yielded 21 hits corresponding to 14 loci
742 (Supplementary Figure 3). Nuclear receptors play key roles in metamorphosis in
743 both insects and some vertebrates, potentially acting in the internal transmission of
744 metamorphosis signals rather than their external reception. Of the 14, seven were
745 upregulated at 133hpf and all of these mRNAs appear to be cleared at the 3-6hpi
746 transition so could have roles in the cue recognition pathway and/ or metamorphosis.
747
748 The *Acropora* developmental transcriptome data, together with the DEView app,
749 have provided novel insights into early coral development and allowed identification

750 of candidate genes for key roles. We hope that the availability of this app via the web
751 will lead to more extensive exploration of the data and ultimately facilitate much
752 better understanding of the molecular processes underlying the development of the
753 coral body plan.
754
755 For a range of organisms, including some corals, considerably more advanced
756 genomic and transcriptomic resources are now available than could have been
757 imagined even a few years ago. However, despite the developmental transcriptomic
758 data provided here being to our knowledge the most comprehensive available for
759 any coral, users need to be aware that the quality of the *Acropora millepora* dataset
760 falls short of those available for the model invertebrates *Drosophila* and
761 *Caenorhabditis*. Nevertheless, the developmental novelties uncovered here provide
762 clear indications of how useful the dataset can be in facilitating coral developmental
763 research.
764
765 **Acknowledgements**
766
767 The authors gratefully acknowledge the support of the Australian Research
768 Council under Discovery Grant DP170104734, SuperScience Grant (round 2)
769 FS110200046 and Centres of Excellence Grant CE14100020. We also thank
770 Gergely Torda and the staff of the Orpheus Island Research Centre for fieldwork
771 assistance. Some of the in situ images presented here were produced by Lauretta
772 Grasso and Nikki Hislop.
773
774
775

References

Aeschimann F, Neagu A, Rausch M, Großhans H. *let-7* coordinates the transition to adulthood through a single primary and four secondary targets. Life Sci Alliance. 2019; 2(2):e201900335.

Attenborough RMF, Hayward DC, Wiedemann U, Foret S, Miller DJ, Ball EE. Expression of the neuropeptides RFamide and LWamide during development of the coral Acropora millepora in relation to settlement and metamorphosis. Dev Biol. 2019; 446: 56-67.

Aviv T, Lin Z, Lau S, Rendl LM, Sicheri F, Smibert CA. The RNA-binding SAM domain of Smaug defines a new family of post-transcriptional regulators. Nat Struct Biol. 2003;10(8):614-21.

Ayers TN, Nicotra ML, Lee MT. Parallels and contrasts between the cnidarian and bilaterian maternal-to-zygotic transition are revealed in Hydractinia embryos. PLoS Genet. 2023;19(7):e1010845.

Ball EE, Hayward DC, Bridge TCL, Miller DJ. *Acropora* – the most studied coral genus. In: Boutet A, Schierwater B (eds). Handbook of Marine Model Organisms in Experimental Biology - Established and Emerging. 2021. Boca Raton (FL): CRC Press. p. 173-193. DOI: 10.1201/9781003217503-10.

Ball E, Hayward D, Reece-Hoyes J, Hislop N, Samuel G, Saint R, Harrison P and Miller, D. Coral development: from classical embryology to molecular control. Int J Dev Biol. 2002;46:671-678.

Ball EE, Hayward DC, Saint R, Miller, DJ. A simple plan—cnidarians and the origins of developmental mechanisms. Nat Rev Genetics. 2004;*5*(8):567-577.

Bamberger C, Pankow S, Yates JR 3rd. Nvp63 and nvPIWIL1 suppress retrotransposon activation in the sea anemone Nematostella vectensis. J Proteome Res. 2022; 21(11):2586-2595.

Bartel DP. MicroRNAs: genomics, biogenesis, mechanism, and function. Cell. 2022; 116(2):281-97.

Baugh LR, Hill AA, Slonim DK, Brown EL, Hunter CP. Composition and dynamics of the Caenorhabditis elegans early embryonic transcriptome. Development. 2003; 130(5):889-900.

820 Birrell CL, Mccook LJ, Willis BL, Harrington L. Chemical effects of macroalgae on
821 larval settlement of the broadcast spawning coral Acropora millepora. Mar Ecol Prog
822 Ser. 2008;362:129–137.
823
824 Bou-Abdullah F, Chasteen ND, Lesser MP. Quenching of superoxide radicals by
825 green fluorescent protein. Biochim Biophys Acta. 2006;1760(11):1690-5.
826
827 Breitwieser FP, Baker DN, Salzberg SL. KrakenUniq: confident and fast
828 metagenomics classification using unique k-mer counts. Genome Biol. 2018;19:198.
829
830 Chen L, Dumelie JG, Li X, Cheng MH, Yang Z, Laver JD, Siddiqui NU, Westwood
831 JT, Morris Q, Lipshitz HD, Smibert CA. Global regulation of mRNA translation and
832 stability in the early Drosophila embryo by the Smaug RNA-binding protein. Genome
833 Biol. 2014;15(1):R4.
834
835 Chen S, Zhou Y, Chen Y, Gu J. fastp: an ultra-fast all-in-one FASTQ preprocessor.
836 Bioinformatics. 2018;34:i884-i890.
837
838 Chille E, Strand E, Neder M, Schmidt V, Sherman M, Mass T, Putnam H.
839 Developmental series of gene expression clarifies maternal mRNA provisioning and
840 maternal-to-zygotic transition in a reef-building coral. BMC Genomics. 2021;
841 22(1):815.
842
843 Clarke DN, Rose NH, De Meulenaere E, Rosental B, Pearse JS, Pearse VB, Deheyn
844 DD Fluorescent proteins generate a genetic color polymorphism and counteract
845 oxidative stress in intertidal sea anemones. Proc Natl Acad Sci USA. 2024;
846 121(11):e2317017121.
847
848 Di Tommaso P, Chatzou M, Floden EW, Barja PP, Palumbo E, Notredame C.
849 Nextflow enables reproducible computational workflows. Nat Biotechnol. 2017;
850 35:316-319.
851
852 Fridrich A, Modepalli V, Lewandowska M, Aharoni R, Moran Y.) Unravelling the
853 developmental and functional significance of an ancient Argonaute duplication. Nat
854 Commun. 2020;11(1):6187.
855
856 Gerber AP, Luschnig S, Krasnow MA, Brown PO, Herschlag D. Genome-wide
857 identification of mRNAs associated with the translational regulator PUMILIO in
858 Drosophila melanogaster. Proc Natl Acad Sci USA. 2006;103(12):4487-92.
859
860 Gilbert E, Craggs J, Modepalli V. Gene Regulatory Network that Shaped the
861 Evolution of Larval Apical Organ in Cnidaria. Mol Biol Evol. 2024;41: msad285.
862

Grasso L, Maindonald J, Rudd S, Hayward D, Saint R, Miller DJ, Ball EE. Microarray analysis provides candidate genes for key roles in coral development. BMC Genomics. 2008;9:540.

Grasso LC, Negri AP, Foret S, Hayward DC, Miller DJ, Ball EE. The biology of coral metamorphosis: molecular responses of coral larvae to inducers of settlement and metamorphosis. Dev Biol. 2011;353:411-419.

Gu Z, Hübschmann D. Make Interactive Complex Heatmaps in R. Bioinformatics. 2022;38:1460–1462. https://doi.org/10.1093/bioinformatics/btab806.

Hadfield MG. Biofilms and Marine Invertebrate Larvae: What Bacteria Produce That Larvae Use to Choose Settlement Sites. Ann Rev Marine Sci. 2011;3:453-470.

Hadfield MG. Why and how marine-invertebrate larvae metamorphose so fast. Sem Cell Dev Biol. 2000;11(6):437-443.

Hayward DC, Miller DJ, Ball EE. Snail expression during embryonic development of the coral *Acropora*: Blurring the diploblast / triploblast divide? Development Genes and Evolution. 2004;214:257-260.

Hayward DC, Samuel G, Pontynen PC, Catmull J, Saint RB, Miller DJ, Ball EE. Localized expression of a DPP/BMP2-4 ortholog in a coral embryo. Proc Natl Acad Sci USA. 2002;99:8106-8111.

Hayward DC, Hetherington S, Behm CA, Grasso L, Foret S, Miller DJ, Ball EE. Differential gene expression at coral settlement and metamorphosis – a subtractive hybridization study. PLoS One. 2011;6: e26411.

Hayward DC, Grasso LC, Saint RB, Miller DJ, Ball EE. The organizer in evolution: Gastrulation and organizer gene expression highlight the importance of Brachyury during development of the coral *Acropora millepora*. Dev Biol. 2015;399:227-247.

He S, Rangel-Huerta E, Hill E, Ellington L, Chen S, Robb S, Majerová E, Drury C, Gibson MC. An evolutionarily conserved Hox-Gbx segmentation code in the rice coral, *Montipora capitata*. bioRxiv preprint. 2024; doi: https://doi.org/10.1101/2024.09.29.615694.

Herchenröther A, Wunderlich TM, Lan J, Hake SB. Spotlight on histone H2A variants: From B to X to Z. Sem Cell Dev Biol. 2023;135:3-12.

Huffmyer AS, Wong KH, Becker DM, Strand E, Mass T, Putnam HM. Shifts and critical periods in coral metabolism reveal energetic vulnerability during development. Curr Biol. 2025;35:1-14;doi https://doi.org/10.1016/j.cub.2025.05.013.

Ishii Y, Hatta M, Deguchi R, Kawata M, Maruyama S. Gene expression alterations from reversible to irreversible stages during coral metamorphosis. Zool Lett. 2022; 8(1):4.

Iwao K, Fujisawa T, Hatta M. A cnidarian neuropeptide of the GLWamide family induces metamorphosis of reef-building corals in the genus Acropora. Coral Reefs. 2002;21:127-129.

Jessop P, Ruzov A, Gering M. Developmental Functions of the Dynamic DNA Methylome and Hydroxymethylome in the Mouse and Zebrafish: Similarities and Differences. Front Cell Dev Biol. 2018;20(6):27.

Jones P, Binns D, Chang HY, Fraser M, Li W, McAnulla C, McWilliam H, Maslen J, Mitchell A, Nuka G, Pesseat S. InterProScan 5: genome-scale protein function classification. Bioinformatics. 2014;30(9):1236-40.

Kitamura M, Koyama T, Nakano Y, Uemura D. Characterization of a natural inducer of coral larval metamorphosis. J Exp Mar Biol Ecol. 2007;340:96-102.

Kitamura M, Schupp PJ, Nakano Y, Uemura D. Luminaolide, a novel metamorphosis-enhancing macrodiolide for scleractinian coral larvae from crustose coralline algae. Tetrahedron Letts. 2009;50:6606-6609.

Langfelder P, Horvath S. WGCNA: an R package for weighted correlation network analysis. BMC Bioinformatics. 2008;9:559. https://doi.org/10.1186/1471-2105-9-559.

Langmead B, Salzberg SL. Fast gapped-read alignment with Bowtie 2. Nat Methods. 2012;9:357-359.

Levy S, Elek A, Grau-Bové X, Menéndez-Bravo S, Iglesias M, Tanay A, Mass T, Sebé-Pedrós A. A stony coral cell atlas illuminates the molecular and cellular basis of coral symbiosis, calcification, and immunity. Cell. 2021;184(11):2973-2987.

Li B, Dewey CN. RSEM: accurate transcript quantification from RNA-Seq data with or without a reference genome. BMC Bioinformatics. 2011;12:323.

Lorković ZJ, Berger F. Heterochromatin and DNA damage repair: Use different histone variants and relax. Nucleus. 2017;8(6):583-588.

Love MI, Huber W, Anders S. Moderated estimation of fold change and dispersion for RNA-seq data with DESeq2. Genome Biol. 2014;15:550.

Mansour TA, Rosenthal JJ, Brown CT, Roberson LM. Transcriptome of the Caribbean stony coral Porites astreoides from three developmental stages. Gigascience. 2016;5(1):33.

Mason BM, Cohen JH. Long-wavelength photosensitivity in coral planula larvae. Biol Bull. 2012;222(2):88-92.

Mason B, Cooke I, Moya A, Augustin R, Lin M-F, Satoh N, Bosch TCG, Bourne DG, Hayward DC, Andrade N, Forêt S, Ying H, Ball EE, Miller DJ. AmAMP1 from *Acropora millepora* and damicornin define a family of coral-specific antimicrobial peptides related to the Shk toxins of sea anemones. Dev Comp Immunol. 2021;114: 103866.

Mason B, Hayward DC, Moya A, Cooke I, Sorenson A, Brunner R, Andrade N, Huerlimann R, Bourne DG, Schaeffer P, Grinblat M, Ravasi T, Ueda N, Tang SL, Ball EE, Miller DJ. Microbiome manipulation by corals and other Cnidaria via quorum quenching. Curr Biol. 2024;34(14):3226-3232.e5.

Mason BM, Koyanagi M, Sugihara T, Iwasaki M, Slepak V, Miller DJ, Sakai Y, Terakita A. Multiple opsins in a reef-building coral, *Acropora millepora*. Scientific Reports 2023;23:1628.

Matsumoto N, Sato K, Nishimasu H, Namba Y, Miyakubi K, Dohmae N, Ishitani R, Siomi H, Siomi MC, Nureki O. Crystal structure and activity of the endoribonuclease domain of the piRNA pathway factor Maelstrom. Cell Reps. 2015;11:366-375.

Mazza ME, Pang K, Reitzel AM, Martindale MQ, Finnerty JR. A conserved cluster of three PRD-class homeobox genes (homeobrain, rx and orthopedia) in the Cnidaria and Protostomia. EvoDevo. 2010;1:1-15.

Meyer E, Aglyamova GV, Matz MV. Profiling gene expression responses of coral larvae (Acropora millepora) to elevated temperature and settlement inducers using a novel RNA-Seq procedure. Mol Ecol. 2011;20:3599-616.

Meyer E, Aglyamova GV, Wang S, Buchanan-Carter J, Abrego D, Colbourne JK, Willis BL, Matz MV. Sequencing and de novo analysis of a coral larval transcriptome using 454 GSFlx. BMC Genomics. 2009;10:1-8.

Michail C, Rodrigues Lima F, Viguier M, Deshayes F. Structure and function of the lysine methyltransferase SETD2 in cancer: From histones to cytoskeleton. Neoplasia. 2025;59:101090.

992 Miller DJ, Hemmrich G, Ball EE, Hayward DC, Khalturin K, Funayama N, Agata K,
993 Bosch TCG.The innate immune repertoire in Cnidaria – ancestral complexity and
994 stochastic gene loss. Genome Biol. 2007;8:R59.
995
996 Mishima Y, Tomari Y. Pervasive yet nonuniform contributions of Dcp2 and Cnot7 to
997 maternal mRNA clearance in zebrafish. Genes Cells. 2017;22(7):670-678.
998
999 Modepalli V, Fridrich A, Agron M, Moran Y. The methyltransferase HEN1 is required
1000 in Nematostella vectensis for microRNA and piRNA stability as well as larval
1001 metamorphosis. PLoS Genet. 2018;14(8):e1007590.
1002
1003 Mohr F, Döhner K, Buske C, Rawat VP. TET genes: new players in DNA
1004 demethylation and important determinants for stemness. Exp Hematol. 2011;
1005 39(3):272-81.
1006
1007 Moran Y, Agron M, Praher D, Technau U. The evolutionary origin of plant and animal
1008 microRNAs. Nat Ecol Evol. 2017;1(3):27.
1009
1010 Morse DE, Hooker N, Morse AN, Jensen RA. Control of larval metamorphosis and
1011 recruitment in sympatric agariciid corals. J Exp Mar Biol Ecol. 1988;116(3):193-217.
1012
1013 Negri AP, Webster NS, Hill RT, Heyward AJ. Metamorphosis of broadcast spawning
1014 corals in response to bacteria isolated from crustose algae. Mar Ecol Prog Ser.
1015 2001;*223*:121-131.
1016
1017 Okubo N, Hayward DC, Forêt S, Ball EE. A comparative view of early development
1018 in the corals *Favia lizardensis*, *Ctenactis echinata*, and *Acropora millepora* -
1019 morphology, transcriptome, and developmental gene expression. BMC Evol Biol.
1020 2016;16:1-12.
1021
1022 Okubo N, Mezaki T, Nozawa Y, Nakano Y, Lien YT, Fukami H, Hayward DC, Ball EE
1023 Comparative embryology of eleven species of stony corals (Scleractinia). PLoS One.
1024 2013;8(12): e84115.
1025
1026 Osakabe A, Molaro A Histone renegades: Unusual H2A histone variants in plants
1027 and animals. Sem Cell Dev Biol. 2023;135:35-42.
1028
1029 Palmer CV, Modi CK, Mydlarz LD. Coral fluorescent proteins as antioxidants. PLoS
1030 One. 2009;4(10):e7298.
1031
1032 Praher D, Zimmermann B, Genikhovich G, Columbus-Shenkar Y, Modepalli V,
1033 Aharoni R, Moran Y, Technau U. Characterization of the piRNA pathway during
1034 development of the sea anemone Nematostella vectensis. RNA Biol. 2017;
1035 14(12):1727-1741.

Quinlan ZA, Bennett MJ, Arts MGI, Levenstein M, Flores D, Tholen HM, Tichy L, Juarez G, Haas AF, Chamberland VF, Latijnhouwers KRW, Vermeij MJA, Johnson AW, Marhaver KL, Kelly LW. Coral larval settlement induction using tissue-associated and exuded coralline algae metabolites and the identification of putative chemical cues. Proc Roy Soc B. 2023;290:20231476. https://doi.org/10.1098/rspb.2023.1476.

Rabani M, Pieper L, Chew G-L, Schier AH. A Massively Parallel Reporter Assay of 3' UTR Sequences Identifies In Vivo Rules for mRNA Degradation. Mol Cell. 2017; 68(6):1083-1094.e5.

Reyes-Bermudez A, Desalvo MK, Voolstra CR, Sunagawa S, Szmant AM, Iglesias-Prieto R, Medina M. Gene expression microarray analysis encompassing metamorphosis and the onset of calcification in the scleractinian coral Montastraea faveolata. Mar Genomics 2009;2:149-159.

Ramon-Mateu J, Ferraioli A, Teixidó N, Domart-Coulon I, Houliston E, Copley RR. Aboral cell types of Clytia and coral larvae have shared features and link taurine to the regulation of settlement. Science Adv. 2025;16;11(20):eadv1159.

Reyes-Bermudez A, Villar-Briones A, Ramirez-Portilla C, Hidaka M, Mikheyev AS Developmental Progression in the Coral *Acropora digitifera* Is Controlled by Differential Expression of Distinct Regulatory Gene Networks. Genome Biol Evol. 2016;8(3):851-70.

Salih A, Larkum A, Cox G, Kuhl M, Hoegh-Guldberg Fluorescent pigments in corals are photoprotective. Nature.2000;408:850-853.

Shoguchi E, Beedessee G, Hisata K, Tada I, Narisoko H, Satoh N, Kawachi M, Shinzato C. A New Dinoflagellate Genome Illuminates a Conserved Gene Cluster Involved in Sunscreen Biosynthesis. Genome Biol Evol. 2021;13:evaa235.

Sato K, Siomi MC. Functional and structural insights into the piRNA factor Maelstrom. FEBS Lett. 2015;589:1688-1693.

Siboni N, Abrego D, Puill-Stephan E, King WL, Bourne DG, Raina J-B, Seymour JR, Harder T. Crustose coralline algae that promote coral larval settlement harbor distinct surface bacterial communities. Coral Reefs 2020;39:1703–1713.

Spike CA, Tsukamoto T, Greenstein D. Ubiquitin ligases and a processive proteasome facilitate protein clearance during the oocyte-to-embryo transition in *Caenorhabditis elegans*. Genetics. 2022;221(1):iyac051.

1080 Strader ME, Davies SW, Matz MV (2015) Differential responses of coral larvae to the
1081 colour of ambient light guide them to suitable settlement microhabitat. R Soc Open
1082 Sci 2(10):150358
1083
1084 Strader ME, Aglyamova GV, Matz MV. Molecular characterization of larval
1085 development from fertilization to metamorphosis in a reef-building coral. BMC
1086 Genomics. 2018;19(1):1-17.
1087
1088 Takeuchi T, Yamada L, Shinzato C, Sawada H, Satoh N. Stepwise Evolution of
1089 Coral Biomineralization Revealed with Genome-Wide Proteomics and
1090 Transcriptomics. PLoS One 2016;11(6):e0156424.
1091
1092 Tebben J, Motti CA, Siboni N, Tapiolas DM, Negri AP, Schupp PJ, Kitamura M,
1093 Hatta M, Steinberg PD, Harder T. Chemical mediation of coral larval settlement by
1094 crustose coralline algae. Sci Rep. 2015;5:10803.
1095
1096 Technau U. Gastrulation and germ layer formation in the sea anemone Nematostella
1097 vectensis and other cnidarians. Mech Dev. 2020;163:103628.
1098
1099 Török A, Schiffer PH, Schnitzler CE, Ford K, Mullikin JC, Baxevanis AD, Bacic A,
1100 Frank U, Gornik SG. The cnidarian Hydractinia echinata employs canonical and
1101 highly adapted histones to pack its DNA. Epigenetics Chromatin. 2016;9(1):1-17.
1102
1103 Tran C, Hadfield MG. Are G-protein-coupled receptors involved in mediating larval
1104 settlement and metamorphosis of coral planulae? Biol Bull 2012;222(2):128-36.
1105
1106 Turnlund AC, Vanwonterghem I, Botté ES, Randall CJ, Giuliano C, Kam L, Bell S,
1107 O'Brien P, Negri AP, Webster NS, Lurgi M. Linking differences in microbial network
1108 structure with changes in coral larval settlement. ISME Comm. 2023;3:114.
1109
1110 Vastenhouw NL, Cao WX, Lipshitz HD. The maternal-to-zygotic transition revisited.
1111 Development. 2019;146(11): dev161471
1112
1113 Walker NS, Fernández R, Sneed JM, Paul VJ, Giribet G, Combosch DJ. Differential
1114 gene expression during substrate probing in larvae of the Caribbean coral *Porites*
1115 *astreoides*. Mol Ecol. 2019;28(22):4899-4913.
1116
1117 Wickham H. Data Analysis, in: Wickham, H. (Ed.), Ggplot2: Elegant Graphics for
1118 Data Analysis. Springer International Publishing, Cham, 2016; pp. 189–201.
1119 https://doi.org/10.1007/978-3-319-24277-4_9.
1120
1121 Wu X, Zhang Y. TET-mediated active DNA demethylation: mechanism, function and
1122 beyond. Nat Rev Genet. 2017;18(9):517-534.
1123

Yasuoka Y, Shinzato C, Satoh N. The Mesoderm-Forming Gene brachyury Regulates Ectoderm-Endoderm Demarcation in the Coral Acropora digitifera. Curr Biol. 2016;26(21):2885-2892.

Availability of data and materials

Data accessibility statement: To facilitate use and rapid exploration of the *Acropora millepora* developmental transcriptome we created an interactive web application that is hosted on servers provided by the Australian Research Data Commons Nectar Research Cloud to ensure that it is scalable and highly available for long-term use. Users can access the web application directly at https://amil2dev.mmb.group/ or obtain its source code and the underlying data from our github repository (https://github.com/iracooke/amil2_dev).

Author Contributions

Designed research: AM, DH, BL, EB, DM
Carried out field work: AM, DH, BL, EB
Laboratory work: AM, BL
Performed bioinformatic analyses: SF, AM, DH, IC
Contributed new analytical tools: IC
Analysed the data: AM, RB, MG, DH, DM
Wrote the paper: DH, RB, EB, IC, DM (lead)

Figure legends

Figure 1. Images showing the morphologies recorded at the time of collection at the timepoints indicated. Times are given in hours post fertilisation (hpf) and hours post induction (hpi). The places in the developmental sequence of two major events, gastrulation and induction with a settlement cue, are indicated. Some of the SEM

1157 images have been previously published in Grasso et al. 2008, Hayward et al. 2011,
1158 and Ball et al. 2021.
1159
1160 Figure 2. PCA analysis of the developmental transcriptomic data. Principal
1161 Components Analysis (PCA) of the developmental transcriptome data with ellipses
1162 representing 95% confidence levels. At 93 hours post fertilisation (hpf), larvae were
1163 competent to settle in response to ethanolic CCA extract and settlement was
1164 induced at the age of 133hpf. Settlement induction caused larvae to elongate at 15
1165 minutes post induction (mpi) and 100% of larvae had initiated metamorphosis at 3
1166 hours post induction (hpi). A major change in gene expression occurred between 3
1167 and 6hpi.
1168
1169 Figure 3. Serial up-down expression plots showing the number of genes changing in
1170 expression between consecutive time points during development. There are three
1171 periods that show major changes in expression: early development leading up to
1172 gastrulation (5-29hpf), 81-133hpf as competence to settle is developing, and 3-6hpi
1173 as polyp development is getting under way after settlement.
1174
1175 Figure 4. Expression of histone genes and histone modifying enzymes during the
1176 early development of *Acropora millepora*. (A) Heatmap showing expression of
1177 selected histone genes during development. mRNAs encoding canonical histones
1178 H3, H4 and H2B are present at high levels in eggs (rows 3, 4 and 5 from the top), as
1179 are H2A.X and H2A.V (but not canonical H2A) messages. Zygotic expression of the
1180 four core canonical histones begins at the start of gastrulation (i.e. the 13hpf time
1181 point) note that the set of histone genes shown in the bottom four rows are likely to
1182 represent a replication-dependent subset that may be required at high levels only
1183 early in development. Consistent with this, the top row shows data for another H2A
1184 gene, expression of which begins later in development. (B) Heatmap showing
1185 expression of histone modifying enzymes during the early development of *Acropora*.
1186 mRNAs encoding the histone acetyltransferase KAT6A the histone H3K36
1187 methylase SETD2 are maternal (rows 2 and 3, respectively). Two other histone
1188 acetyltransferases (HAC5 and KAT5; top and bottom rows) are most highly
1189 expressed at the 6hpi time point, reflecting their possible role in activating chromatin

1190 during the post-settlement transition. Note that a second wave of expression of both
1191 KAT6A and SETD2 also occurs at that time.
1192
1193 Figure 5. Heatmaps and in situ hybridisation provide complementary data, as
1194 illustrated by data for coral homologs of the *Drosophila* genes, snail and homeobrain.
1195 During gastrulation, these genes have complementary morphological expression
1196 patterns, *Am-snail* marking the presumptive mesendoderm (Hayward et al. 2004)
1197 and *Am-homeobrain* the presumptive ectoderm. (A) Diagrammatic vertical sections
1198 of embryos aged from early prawn chip to sphere. (B-D) Embryos aged from prawn
1199 chip to sphere (blastopore closure) viewed in three different ways. (B) Critical-point
1200 dried embryos viewed with scanning electron microscopy reveal the external
1201 morphology, (C) Whole mount in situ hybridisation reveals the spatial expression of
1202 *Am-snail*. (D) Vertical sections of in situ preparations reveal the internal distribution
1203 of the expressing tissue in the developing mesendoderm. (E) Expression of *Am-*
1204 *homeobrain* in the developing ectoderm revealed using whole-mount in situ
1205 hybridisation. Note that the two genes are complimentary in their expression. (C', E')
1206 Heatmap showing the relative expression of the two corresponding genes over the
1207 course of development. Parts of the figure were published in Hayward et al. (2004)
1208 Development Genes & Evolution 214:257-260, Springer Nature.
1209
1210 Figure 6. In situ hybridisation and heatmaps provide complementary data in support
1211 of roles for known and suspected anti-bacterial activities during settlement and
1212 metamorphosis in *Acropora*. The upper three rows show in situ hybridisation data for
1213 developmental stages leading into and immediately following settlement for (A) the
1214 anti-microbial protein AmAMP1 (Mason et al. (2021), (B) the quorum quenching
1215 activity AmNtNH1 (Mason et al. 2024), and (C) the MAC-Perforin protein Apextrin
1216 Miller et al. 2007; Hayward et al. 2011). A', B' and C' are heatmaps showing the
1217 corresponding temporal expression levels of the three genes. The arrowheads
1218 indicate the time of settlement induction.
1219
1220 Figure 7. Heatmaps for genes implicated in (A) DNA methylation /demethylation and
1221 (B) clearance of mRNAs and proteins are consistent with major changes in gene
1222 activity occurring at 3-6hpi. The upper panel (A) illustrates relative expression levels
1223 of the *Acropora* homologs of ten-eleven-translocase (tet), the primary role of which is

1224 removal of CpG methylation marks, the de novo DNA methyltransferase, DNMT3,
1225 and the maintenance DNA methyltransferase, DNMT1. Although all three activities
1226 are expressed during gastrulation, TET is most heavily expressed at the 6hpi time
1227 point. The lower panel (B) shows relative expression levels of *Acropora* homologs of
1228 the conserved mRNA clearance activities, Smaug and Pumilio, and the TRIM-NHL
1229 ubiquitin ligase, TRIM71/LIN41. Smaug and TRIM71/LIN41are most heavily
1230 expressed at the 6hpi time point; three gene predictions annotated as Pumilio
1231 homologs (corresponding to at least two distinct gene products) were also up-
1232 regulated at that time.
1233
1234 Figure 8. Expression of genes involved in small RNA (miRNA and piRNA)
1235 processing during early development. mRNAs encoding HEN1 and Dicer homologs
1236 (rows 6 and 7) were present at high levels in eggs, as were those encoding
1237 homologs of Maelstrom, Vasa/DDX4.1 and .2, and Piwi2, which function primarily in
1238 piRNA-mediated transposon silencing. Other miRNA processing activities, including
1239 homologs of Serrate/SRRT and DGCR8/Pasha, were also expressed in embryos,
1240 larvae and during post settlement life, implying extensive involvement of miRNAs in
1241 regulating gene activities during early coral development.
1242
1243 Supplementary Figure 1.
1244 Weighted gene co-expression network analysis (WGCNA) clustered the
1245 developmental gene expression data into 39 modules based on correlated
1246 expression patterns. The number of genes in each module range from 18 (plum
1247 module) to 5851 (turquoise module) and the grey module contains all genes that did
1248 not fit into any other module. The WGCNA heatmap indicated that there is a major
1249 change in gene expression between 3 and 6 hours post induction (hpi) and also
1250 showed that settlement induction at the age of 133 hours post fertilisation (hpf) did
1251 not trigger an immediate strong change in gene expression 15 minutes post
1252 induction (mpi).
1253
1254 Supplementary Figure 2.
1255 Genes previously characterised in the context of gastrulation illustrate the need for
1256 spatial as well as temporal expression data. In situ data for the *Acropora* homologs
1257 of several genes imply conservation of function during gastrulation with Bilateria. (A)

1258 BMP2/4 (BMP2B), (B) Forkhead (FOXA2), (C) Goosecoid (GSC) and (D) Brachyury
1259 (TBXT). However, heatmaps show that, for most of these genes, rather than at
1260 gastrulation (around 13 – 18 hpf) the expression maxima occur post-settlement. Only
1261 one of the genes characterised in the context of gastrulation (snail) has a major peak
1262 of expression at the late “prawn chip” (gastrula) stage (Figure 5) – which is
1263 consistent with in situ data (Hayward et al. 2004) suggesting expression throughout
1264 the presumptive mesendoderm. The in situs were previously published in Hayward
1265 et al. (2015) Developmental Biology 399:337-347 (Elsevier).
1266
1267
1268 Supplementary Figure 3.
1269 Differential expression of genes encoding nuclear receptors during coral
1270 development. Searching the *Acropora* data using the terms PF00104 Ligand-binding
1271 domain of nuclear hormone receptor and PF00105 Zinc finger, C4 type (two
1272 domains) yielded hits corresponding to 14 loci. Two of these loci code for predicted
1273 protein isoforms with distinct expression profiles (XP_029208454.1 and
1274 XP_029208455.1 are protein isoforms from the locus LOC114972094;
1275 XP_044184859.1 and XP_044184860.1 are isoforms from the locus
1276 LOC114969161). Consistent with possible roles in cue recognition and/ or
1277 metamorphosis, seven of the 14 genes were upregulated at 133hpf. All of these
1278 mRNAs were cleared at the 3-6hpi transition.
1279

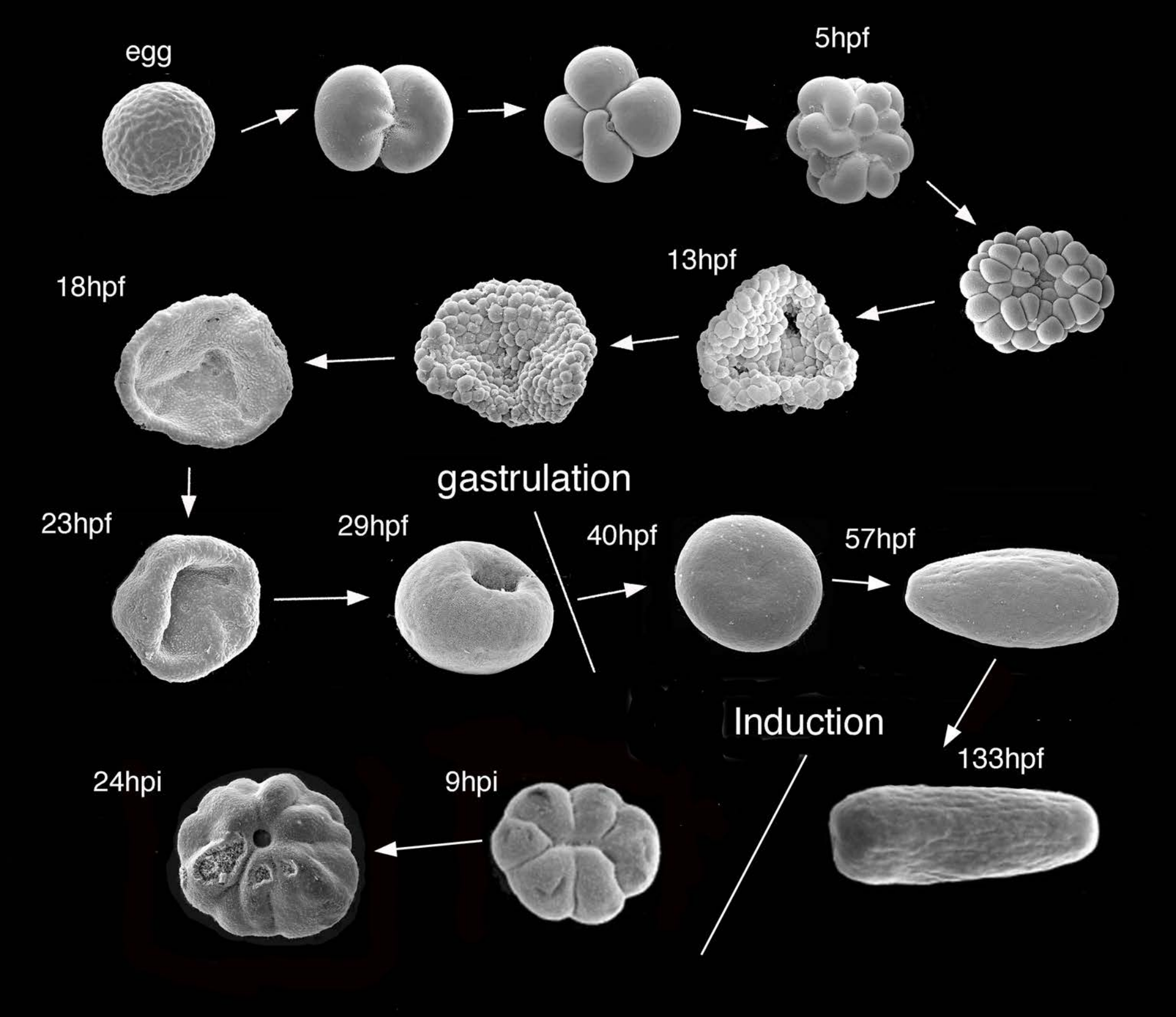
egg
5hpf
13hpf
18hpf
gastrulation
23hpf
29hpf
40hpf
57hpf
Induction
133hpf
24hpi
9hpi

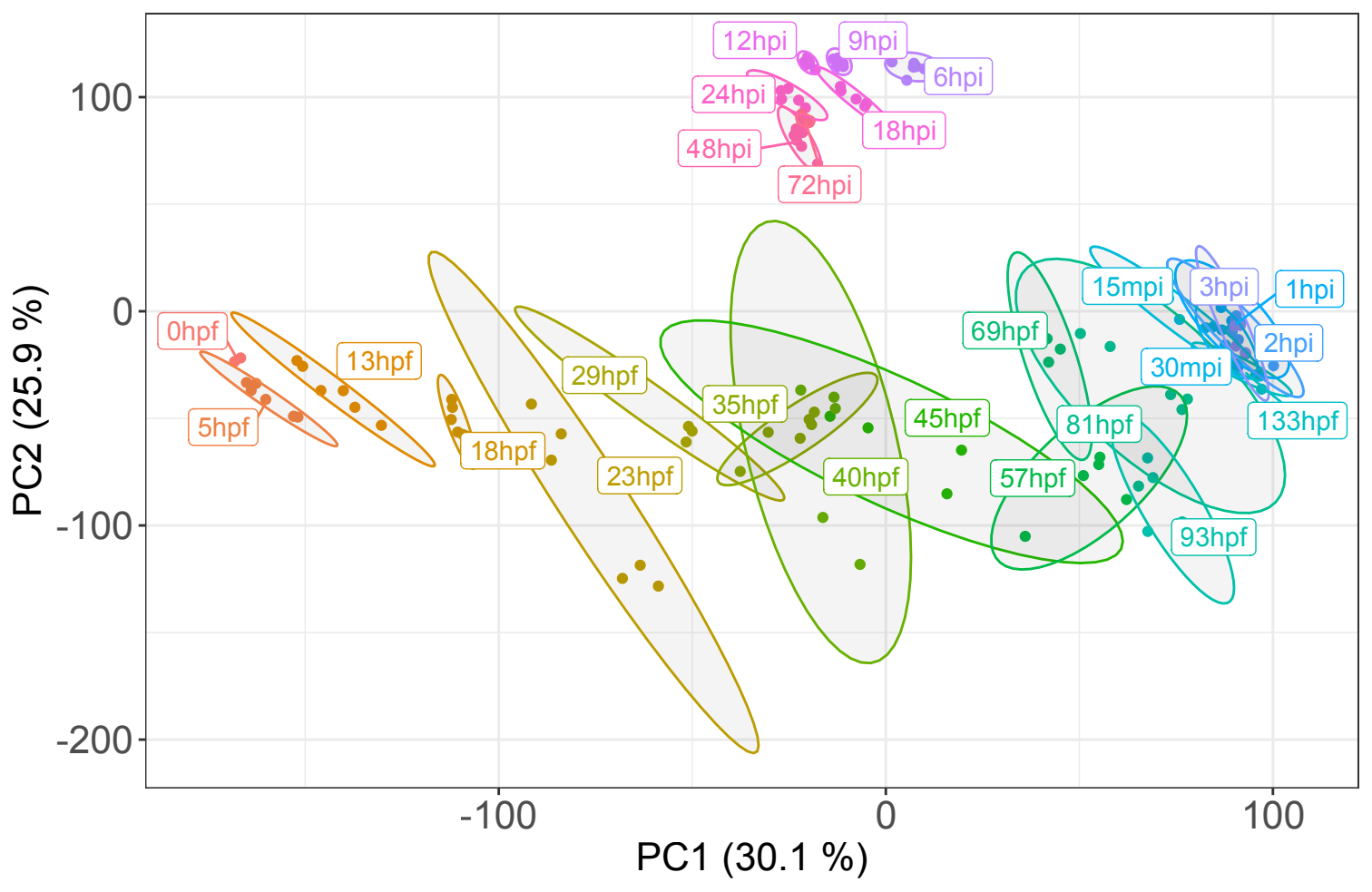
12hpi
9hpi
6hpi
24hpi
18hpi
48hpi
72hpi
0hpf
13hpf
5hpf
18hpf
29hpf
23hpf
35hpf
40hpf
45hpf
69hpf
57hpf
81hpf
93hpf
15mpi
3hpi
1hpi
2hpi
30mpi
133hpf
100
0
-100
-200
-100
0
100
PC2 (25.9 %)
PC1 (30.1 %)

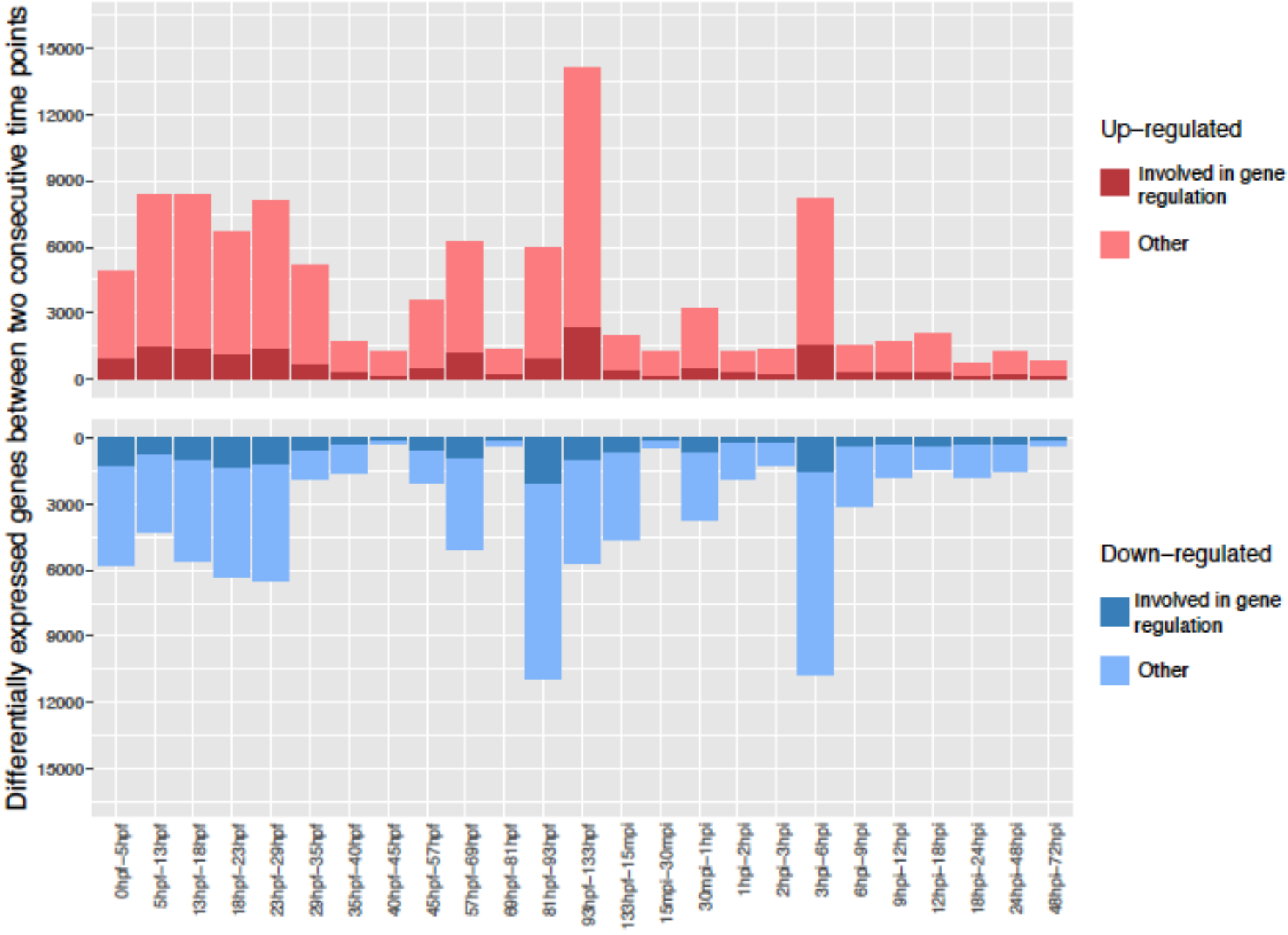
Differentially expressed genes between two consecutive time points
15000
12000
9000
6000
3000
0
Up−regulated
Involved in gene regulation
Other
Down−regulated
Involved in gene regulation
Other
0hpf−5hpf
5hpf−13hpf
13hpf−18hpf
18hpf−23hpf
23hpf−29hpf
29hpf−35hpf
35hpf−40hpf
40hpf−45hpf
45hpf−57hpf
57hpf−69hpf
69hpf−81hpf
81hpf−93hpf
93hpf−133hpf
133hpf−15mpi
15mpi−30mpi
30mpi−1hpi
1hpi−2hpi
2hpi−3hpi
3hpi−6hpi
6hpi−9hpi
9hpi−12hpi
12hpi−18hpi
18hpi−24hpi
24hpi−48hpi
48hpi−72hpi

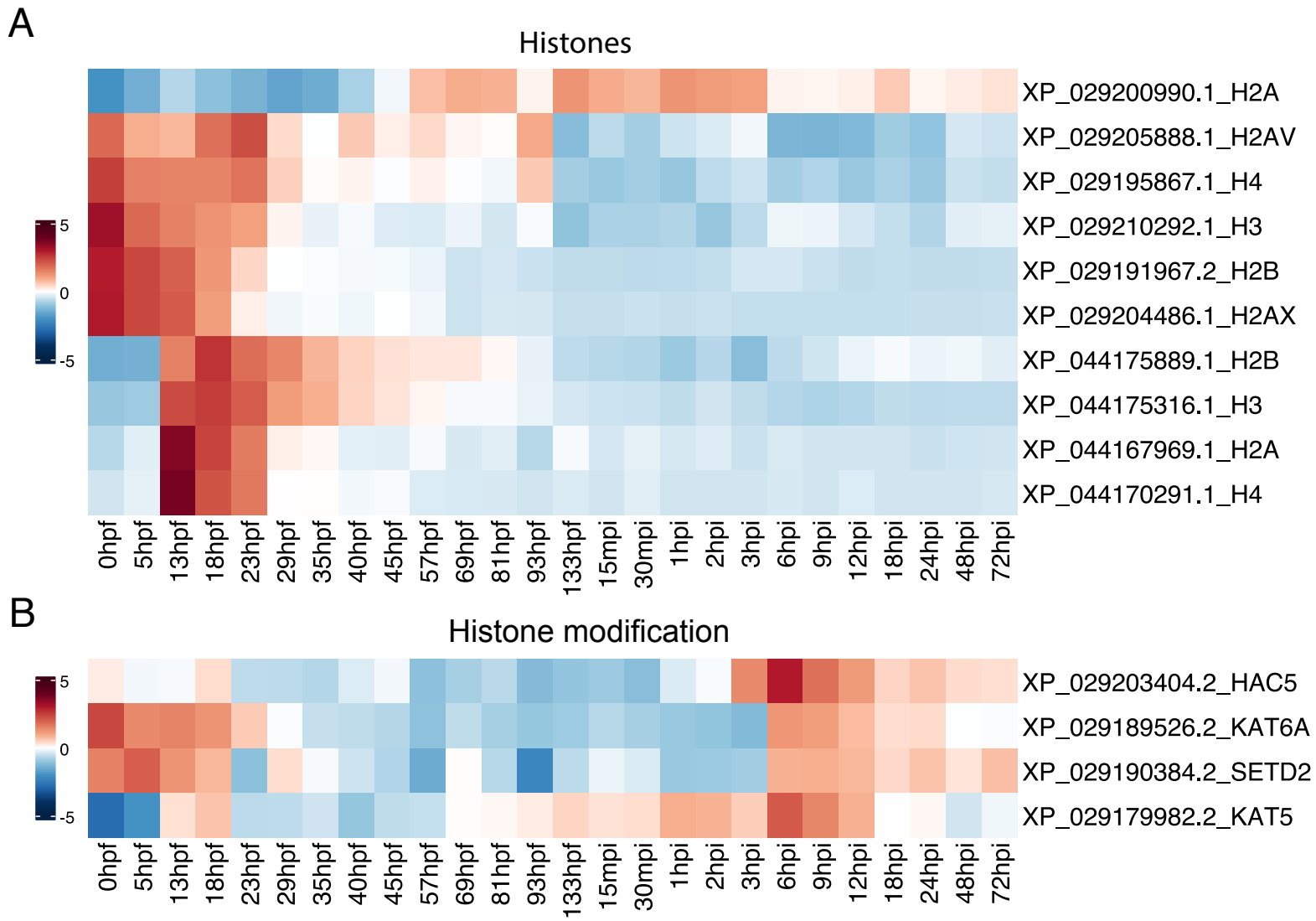
A
Histones
XP_029200990.1_H2A
XP_029205888.1_H2AV
XP_029195867.1_H4
XP_029210292.1_H3
XP_029191967.2_H2B
XP_029204486.1_H2AX
XP_044175889.1_H2B
XP_044175316.1_H3
XP_044167969.1_H2A
XP_044170291.1_H4
5
0
-5
0hpf
5hpf
13hpf
18hpf
23hpf
29hpf
35hpf
40hpf
45hpf
57hpf
69hpf
81hpf
93hpf
133hpf
15mpi
30mpi
1hpi
2hpi
3hpi
6hpi
9hpi
12hpi
18hpi
24hpi
48hpi
72hpi
B
Histone modification
XP_029203404.2_HAC5
XP_029189526.2_KAT6A
XP_029190384.2_SETD2
XP_029179982.2_KAT5
5
0
-5
0hpf
5hpf
13hpf
18hpf
23hpf
29hpf
35hpf
40hpf
45hpf
57hpf
69hpf
81hpf
93hpf
133hpf
15mpi
30mpi
1hpi
2hpi
3hpi
6hpi
9hpi
12hpi
18hpi
24hpi
48hpi
72hpi

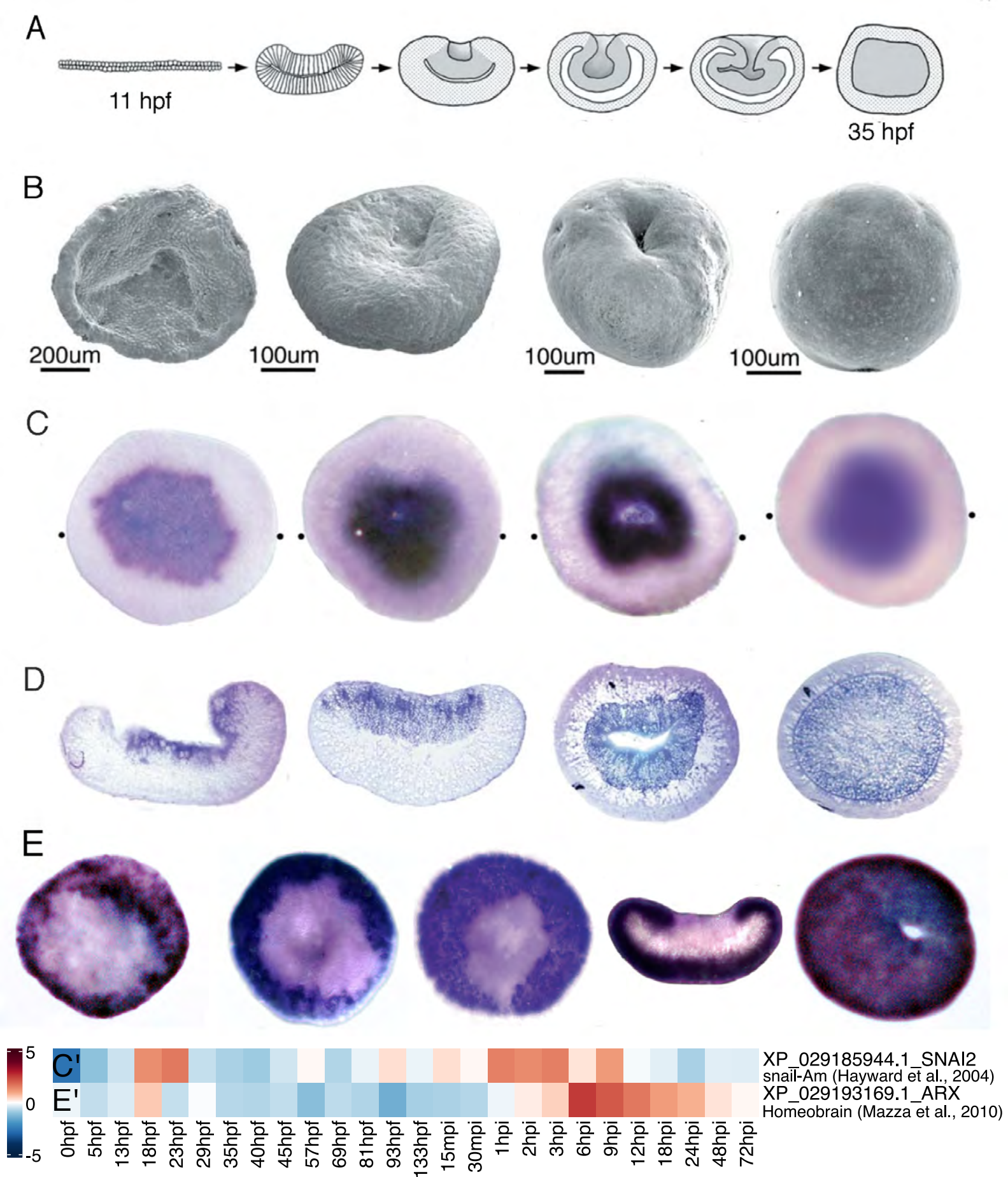
A
11 hpf
35 hpf
B
200um
100um
100um
100um
C
D
E
5
0
-5
C'
E'
0hpf
5hpf
13hpf
18hpf
23hpf
29hpf
35hpf
40hpf
45hpf
57hpf
69hpf
81hpf
93hpf
133hpf
15mpi
30mpi
1hpi
2hpi
3hpi
6hpi
9hpi
12hpi
18hpi
24hpi
48hpi
72hpi
XP_029185944.1_SNAI2
snail-Am (Hayward et al., 2004)
XP_029193169.1_ARX
Homeobrain (Mazza et al., 2010)

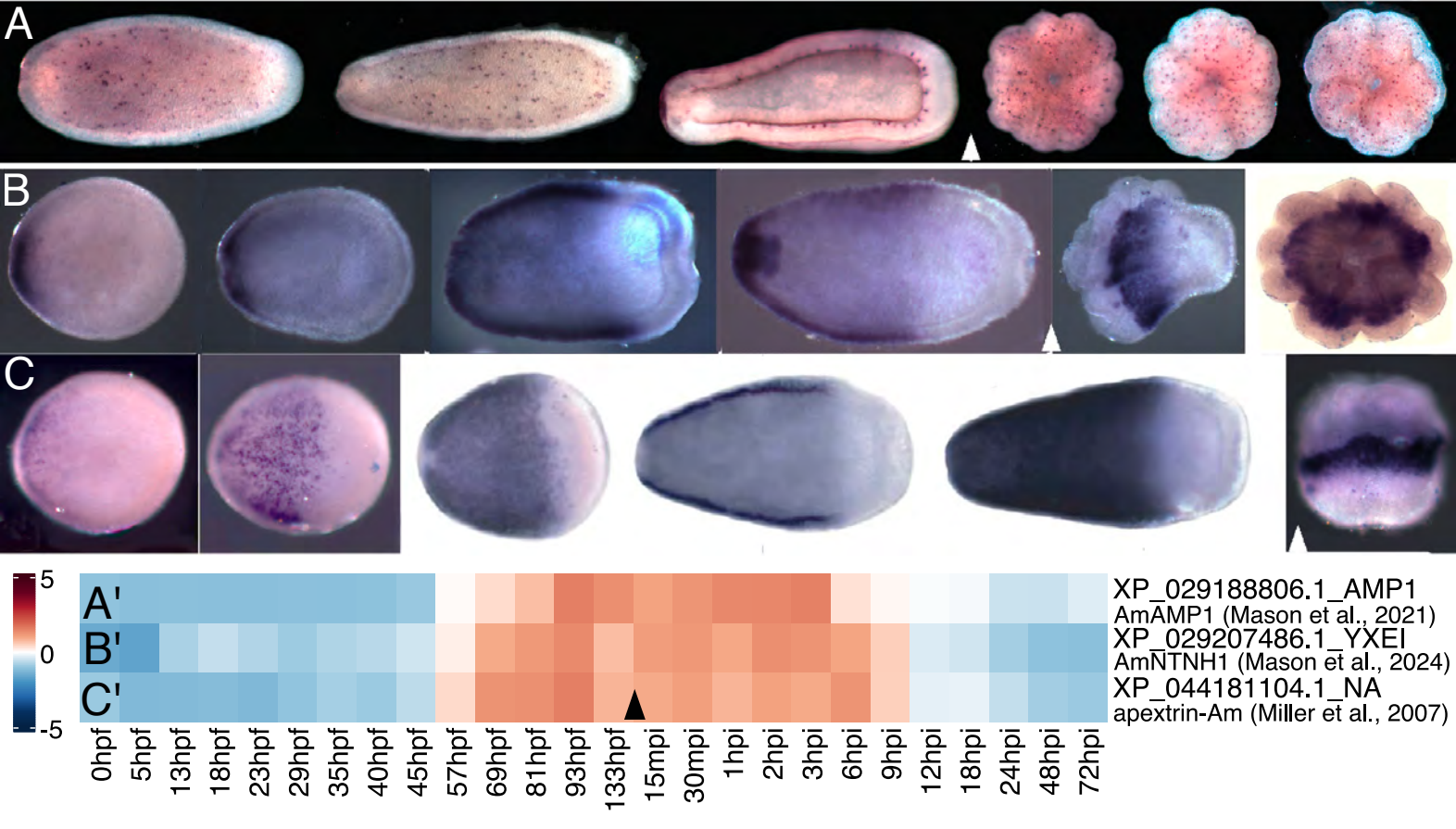
A
B
C
5
0
-5
A'
B'
C'
XP_029188806.1_AMP1
AmAMP1 (Mason et al., 2021)
XP_029207486.1_YXEI
AmNTNH1 (Mason et al., 2024)
XP_044181104.1_NA
apextrin-Am (Miller et al., 2007)
0hpf
5hpf
13hpf
18hpf
23hpf
29hpf
35hpf
40hpf
45hpf
57hpf
69hpf
81hpf
93hpf
133hpf
15mpi
30mpi
1hpi
2hpi
3hpi
6hpi
9hpi
12hpi
18hpi
24hpi
48hpi
72hpi

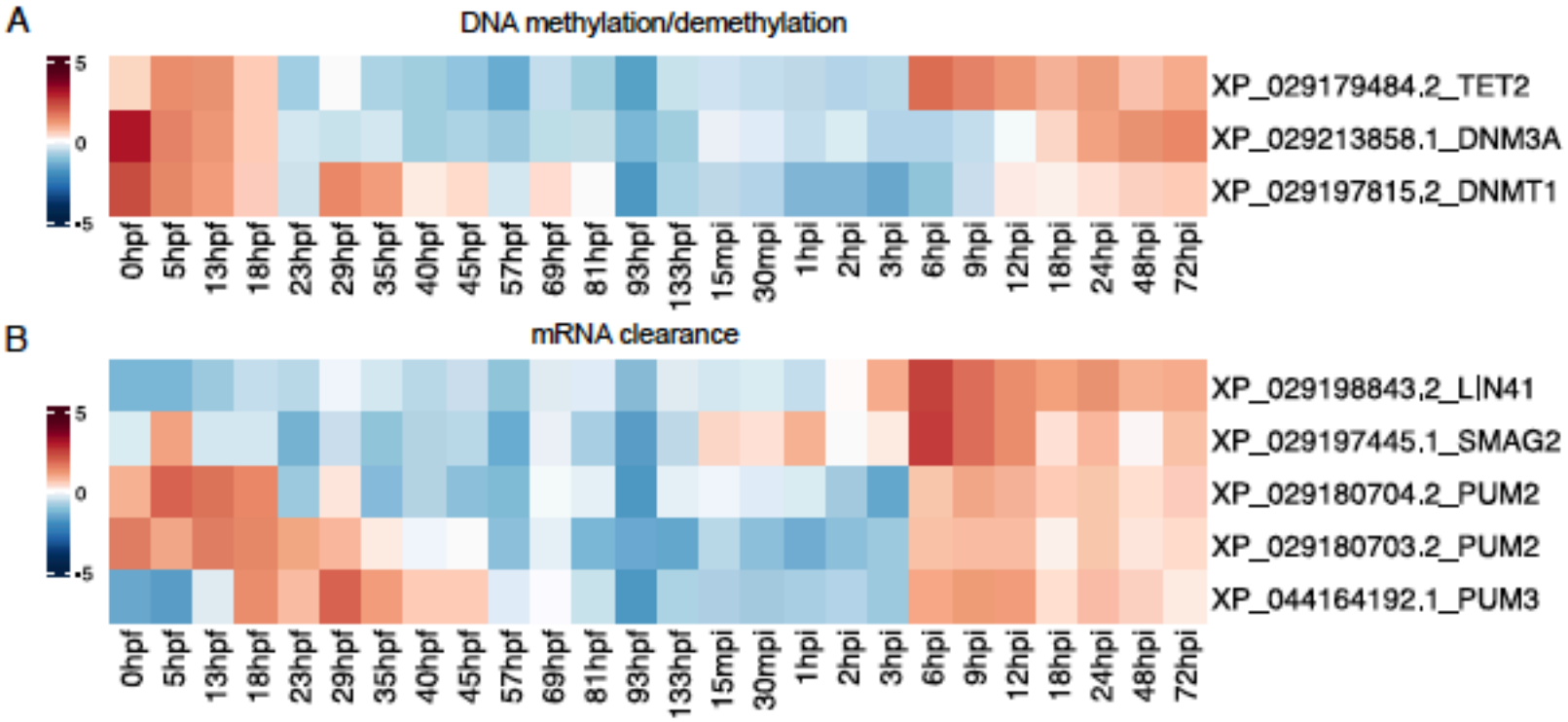
A
DNA methylation/demethylation
5
0
-5
XP_029179484.2_TET2
XP_029213858.1_DNM3A
XP_029197815.2_DNMT1
0hpf
5hpf
13hpf
18hpf
23hpf
29hpf
35hpf
40hpf
45hpf
57hpf
69hpf
81hpf
93hpf
133hpf
15mpi
30mpi
1hpi
2hpi
3hpi
6hpi
9hpi
12hpi
18hpi
24hpi
48hpi
72hpi
B
mRNA clearance
5
0
-5
XP_029198843.2_LIN41
XP_029197445.1_SMAG2
XP_029180704.2_PUM2
XP_029180703.2_PUM2
XP_044164192.1_PUM3
0hpf
5hpf
13hpf
18hpf
23hpf
29hpf
35hpf
40hpf
45hpf
57hpf
69hpf
81hpf
93hpf
133hpf
15mpi
30mpi
1hpi
2hpi
3hpi
6hpi
9hpi
12hpi
18hpi
24hpi
48hpi
72hpi

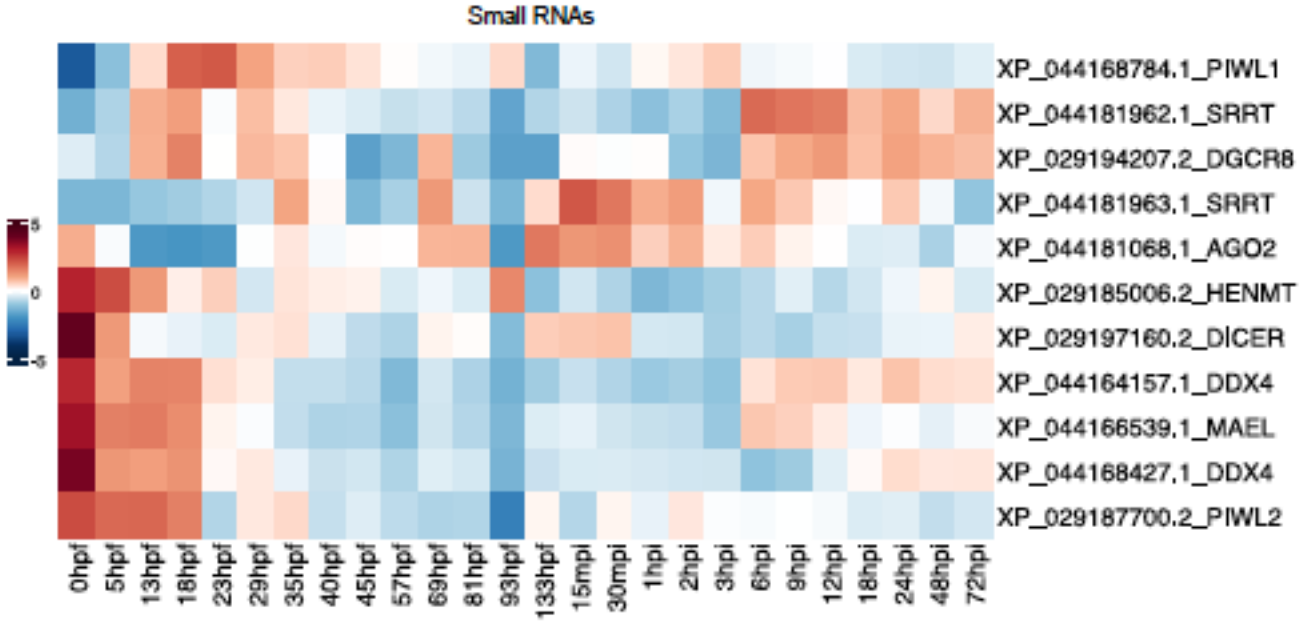
Small RNAs
XP_044168784.1_PIWL1
XP_044181962.1_SRRT
XP_029194207.2_DGCR8
XP_044181963.1_SRRT
XP_044181068.1_AGO2
XP_029185006.2_HENMT
XP_029197160.2_DICER
XP_044164157.1_DDX4
XP_044166539.1_MAEL
XP_044168427.1_DDX4
XP_029187700.2_PIWL2
5
0
-5
0hpf
5hpf
13hpf
18hpf
23hpf
29hpf
35hpf
40hpf
45hpf
57hpf
69hpf
81hpf
93hpf
133hpf
15mpi
30mpi
1hpi
2hpi
3hpi
6hpi
9hpi
12hpi
18hpi
24hpi
48hpi
72hpi

Table 1. Previous studies on the molecular bases of early development in hard corals

Coral species	Reference	Stages sampled						Focus of study	Methodology*
Acropora millepora									
	Grasso et al., 2008	prawn chip 8 hpf	planula 83 hpf	primary polyp 130 hpf	adult			Early survey of developmental changes	ESTs
	Grasso et al., 2011	egg (unfertilised)	prawn chip 8 hpf	planula 83 hpf	primary polyp 130 hpf	adult		Pre- vs post-settlement	ESTs
	Hayward et al., 2011			planula	primary polyp			Pre vs post settlement	SSH
	Strader et al., 2018	22 hpf	46 hpf	73 hpf	89 hpf	24 hour intervals		Competence and fluorescence	
Acropora digitifera									
	Takeuchi et al., 2016	egg	blastula	gastrula	larva	meta	adult	Calcification genes	
	Reyes-Bermudez et al., 2016	prawn chip 12 hpf	gastrula 24 hpf	sphere 48 hpf	planula 96 hpf	adult		Stage specific transcript profiles	
Acropora tenuis									
	Ishii et al. 2022	0, 1 and 6 hr post induction						Commitment to settlement	
Montipora capitata									
	Chillie et al., 2021	0 hpf (egg) (Unfertilised)	1 hpf	4hpf	9hpf	14hpf	22hpf	Maternal-zygotic transition	
	He et al., 2024	0 hpf (egg) (unfertilised?)	prawn chip 14hpf	sphere 38hpf	pear 62hpf	86hpf	planula 110hpf	Developmental roles of Hox-Gbx genes	
	Huffmyer et al., 2025	Egg (fertilised) 1hpf	cleavage 5hpf	late gastrula 38hpf	late gastrula 65hpf	93hpf	183hpf		
Porites asteroides	Walker et al., 2019	Compared pre-competent and competent planulae						Compared non-probing and probing planulae	
	Mansour et al., 2016	Compared pre-settlement, post-settlement and adult						Calcification, settlement and symbiosis	
Montastrea faveolata	Reyes-Bermudez et al., 2009	Planula, primary polyp and adult						Metamorphosis and onset of calcification	Arrays
Stylophora pistllata	Levy et al., 2021	Planula, primary polyp and adult						Characterisation of single cell types	

***With the exception of those where the methodology is specified, these studies were based on high-throughput sequencing data**

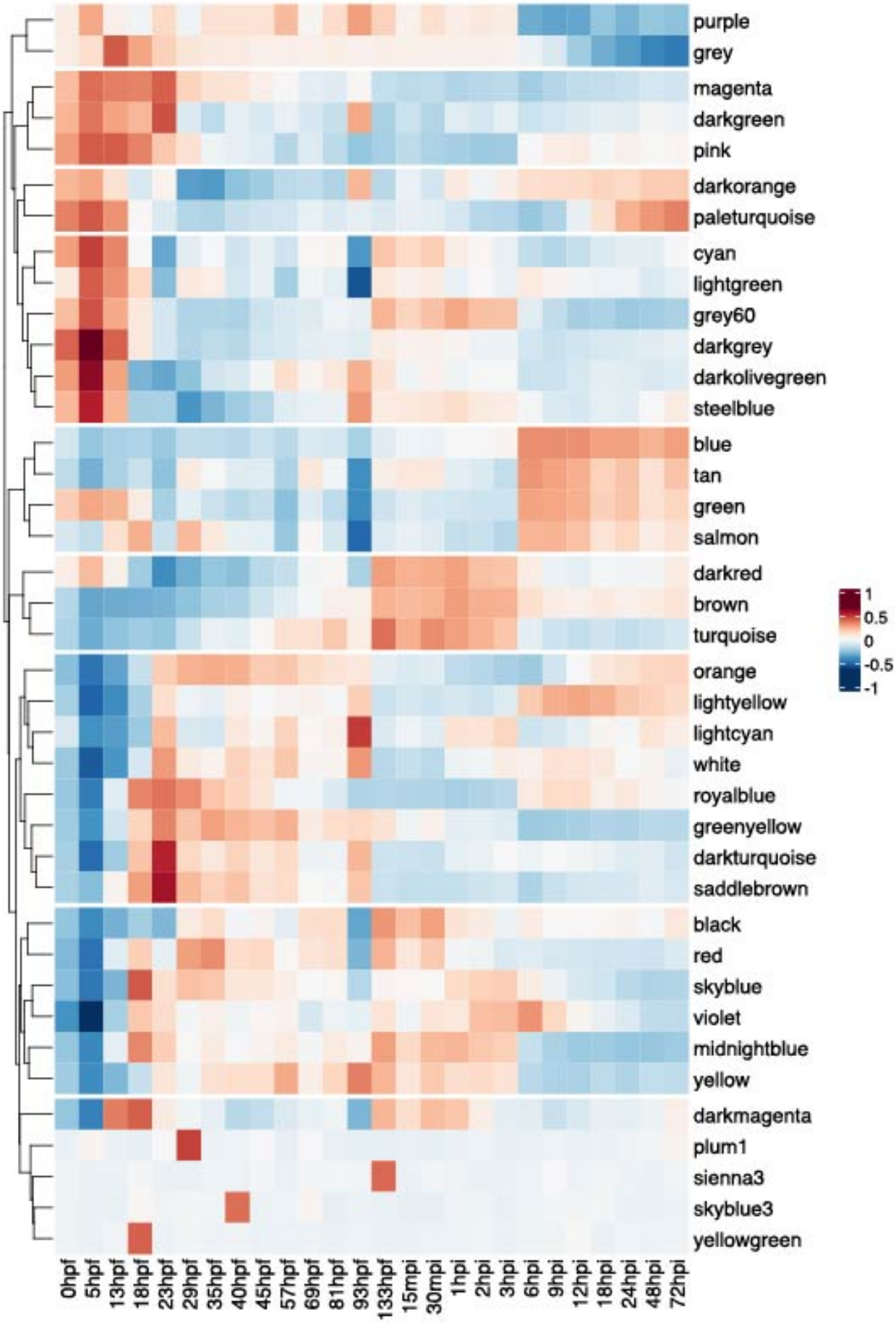
purple
grey
magenta
darkgreen
pink
darkorange
paleturquoise
cyan
lightgreen
grey60
darkgrey
darkolivegreen
steelblue
blue
tan
green
salmon
darkred
brown
turquoise
orange
lightyellow
lightcyan
white
royalblue
greenyellow
darkturquoise
saddlebrown
black
red
skyblue
violet
midnightblue
yellow
darkmagenta
plum1
sienna3
skyblue3
yellowgreen
0hpf
5hpf
13hpf
18hpf
23hpf
29hpf
35hpf
40hpf
45hpf
57hpf
69hpf
81hpf
93hpf
133hpf
15mpi
30mpi
1hpi
2hpi
3hpi
6hpi
9hpi
12hpi
18hpi
24hpi
48hpi
72hpi
1
0.5
0
-0.5
-1

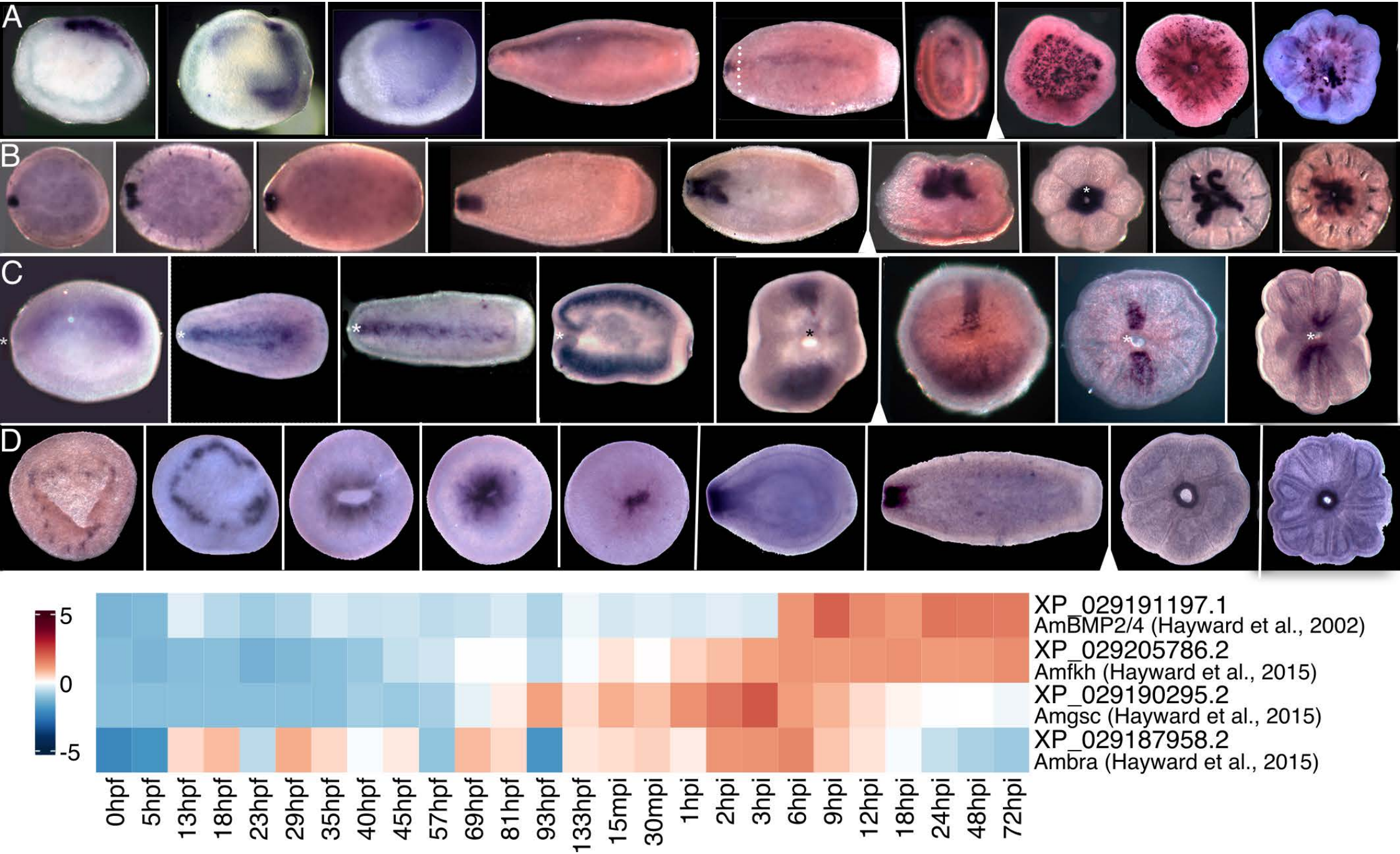
A
B
C
D
5
0
-5
XP_029191197.1
AmBMP2/4 (Hayward et al., 2002)
XP_029205786.2
Amfkh (Hayward et al., 2015)
XP_029190295.2
Amgsc (Hayward et al., 2015)
XP_029187958.2
Ambra (Hayward et al., 2015)
0hpf
5hpf
13hpf
18hpf
23hpf
29hpf
35hpf
40hpf
45hpf
57hpf
69hpf
81hpf
93hpf
133hpf
15mpi
30mpi
1hpi
2hpi
3hpi
6hpi
9hpi
12hpi
18hpi
24hpi
48hpi
72hpi

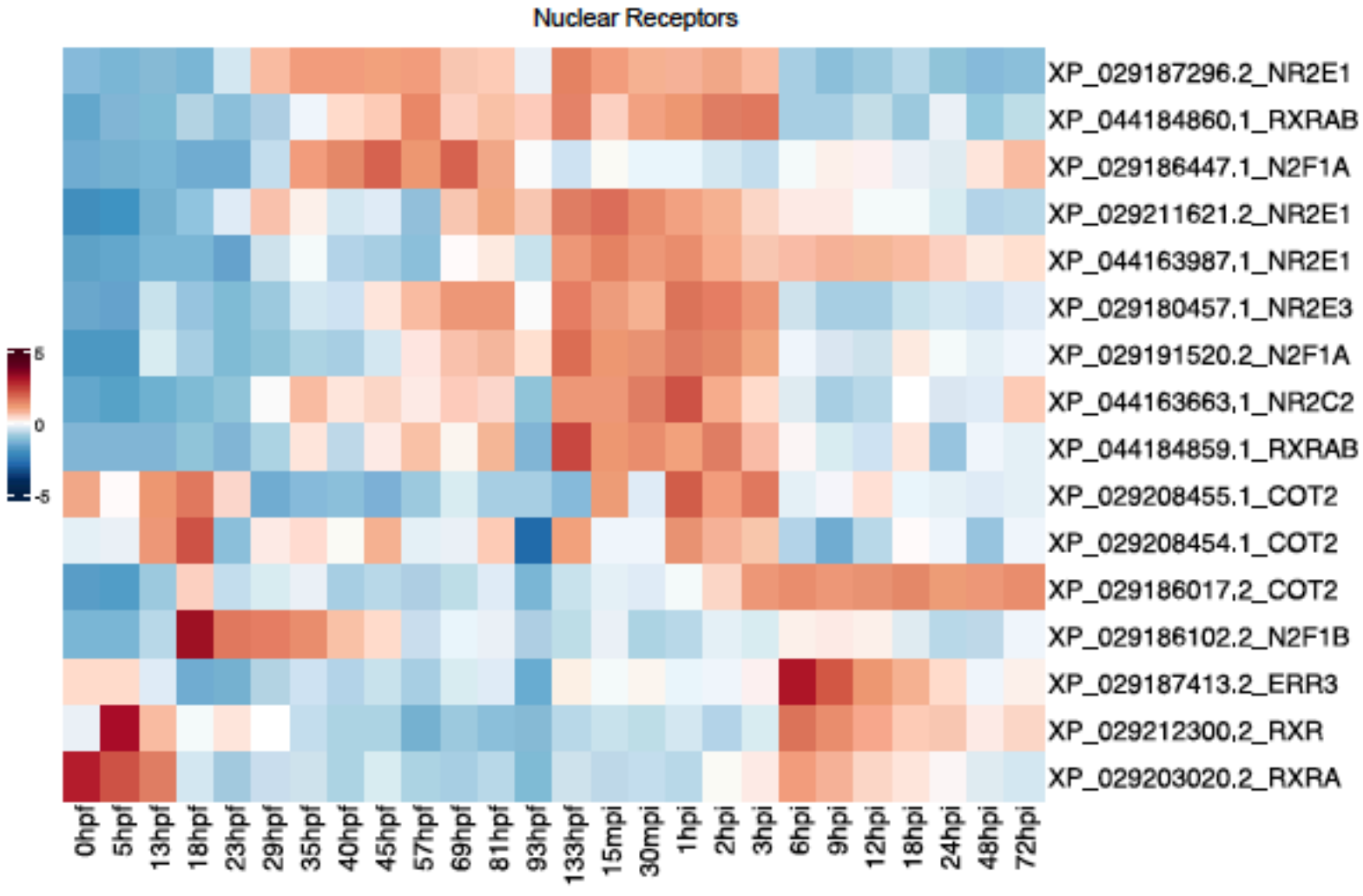
Nuclear Receptors
XP_029187296.2_NR2E1
XP_044184860.1_RXRAB
XP_029186447.1_N2F1A
XP_029211621.2_NR2E1
XP_044163987.1_NR2E1
XP_029180457.1_NR2E3
XP_029191520.2_N2F1A
XP_044163663.1_NR2C2
XP_044184859.1_RXRAB
XP_029208455.1_COT2
XP_029208454.1_COT2
XP_029186017.2_COT2
XP_029186102.2_N2F1B
XP_029187413.2_ERR3
XP_029212300.2_RXR
XP_029203020.2_RXRA
5
0
-5
0hpf
5hpf
13hpf
18hpf
23hpf
29hpf
35hpf
40hpf
45hpf
57hpf
69hpf
81hpf
93hpf
133hpf
15mpi
30mpi
1hpi
2hpi
3hpi
6hpi
9hpi
12hpi
18hpi
24hpi
48hpi
72hpi